Review

Engineering of nanoscale coordination polymers with biomolecules for advanced applications

Jing Mu [a,b,c,1], Liangcan He [c,1], Peng Huang [a,*], Xiaoyuan Chen [c,*]

[a] Guangdong Key Laboratory for Biomedical Measurements and Ultrasound Imaging, Laboratory of Evolutionary Theranostics, School of Biomedical Engineering, Health Science Center, Shenzhen University, Shenzhen 518060, China
[b] Key Laboratory of Optoelectronic Devices and Systems of Ministry of Education and Guangdong Province, College of Optoelectronic Engineering, Shenzhen University, Shenzhen 518060, China
[c] Laboratory of Molecular Imaging and Nanomedicine, National Institute of Biomedical Imaging and Bioengineering, National Institutes of Health, Bethesda, MD 20892, USA

ARTICLE INFO

ABSTRACT

Nanoscale coordination polymers (NCPs) have shown extraordinary advantages in various research areas due to their structural diversity and multifunctionality. Recently, integration of biomolecules with NCPs received extensive attention and the formed hybrid materials exhibit superior properties over the individual NCPs or biomolecules. In this review, the state-of-the-art of approaches to engineer NCPs with different types of guest biomolecules, such as amino acids, nucleic acids, enzymes and lipids are systematically introduced. Additionally, advanced applications of these biomolecule-NCP composites in the areas of sensing, catalysis, molecular imaging and therapy are thoroughly summarized. Finally, current challenges and prospects are also discussed.

Published by Elsevier B.V.

Contents

* Corresponding authors.
  E-mail addresses: peng.huang@szu.edu.cn (P. Huang), shawn.chen@nih.gov (X. Chen).
[1] These authors contributed equally to this work.

1. Introduction

Nanoscale coordination polymers (NCPs) are generally defined as the assembly of metal-containing units and organic linkers *via* metal–ligand coordination interactions. One widely reported subclass of NCPs is nanoscale metal–organic frameworks (NMOFs), which are porous crystalline materials with one-, two-, or three-dimensional structures [1–3]. The past decade has witnessed the progressive development of NCPs, especially NMOFs in various research areas, such as gas storage and separation, catalysis, sensing, energy conversion, and biological applications [4–10]. Due to the diverse choices of metal ions and organic bridging ligands, a plethora of NCPs have been prepared recently. Basically, the intrinsic properties of NMOFs, such as tunable porosity, high surface area and adjustable geometry, *etc.* make them desirable host matrix for a wide range of molecules and nanoparticles [11–13].

Biomolecules, which are widely found in organism to regulate basic life activities, cover a variety of small molecules such as amino acids, fatty acids, *etc.*, and large molecules such as proteins, nucleic acids, carbohydrates and lipids. Advances in science and technology have not only elucidated the biological functions of biomolecules, but also expanded their applications in other fields, such as sensing, imaging, industrial and pharmaceutical uses [14–16]. In general, biomolecules have favored performances in several aspects. For example, they are highly soluble in aqueous solutions, which can be used to adjust the hydrophilic properties of materials. Also, enzymes exhibit high catalytic activity and substrate selectivity. In the industrial area, the biomolecular reactions are usually environmentally friendly and few harmful by-products are produced. In addition, biomolecular modification of nanomaterials has been widely used to overcome a lot of biological barriers, such as targeting for specific cells and organelles or internalization into cells [17–20]. However, there still exist several drawbacks, including their low operational stability, sensitivity to environmental changes and difficulties in recycling, which have severely impeded their further applications. As a result, it is necessary to develop strategies to effectively stabilize biomolecules while maintaining their structures and functions during the engineering process.

Due to the unique physical and chemical properties of NCPs, the integration of biomolecules into NCPs has become a trend in past few years [21–24]. Compared to other nanomaterials (*e.g.* hydrogels, mesoporous silica) for immobilizing biomolecules, NCPs exhibit several unique advantages: 1) The diverse composition, geometry and properties could be customized according to the different purposes [25]; 2) High surface area and tunable porosity could facilitate the high loading capacity of biomolecules. Also, the porous structure allows the easy molecular diffusion and transport between the inner and outer compartments; 3) The synthesis or modifications of NCPs are usually carried out under mild conditions, which could potentially avoid the damage to the structure and function of biomolecules; 4) NCPs are usually formed *via* the coordination bonds, which are relatively degradable under biological conditions. Therefore, the combination of NCPs with biomolecules not only benefits the performances of biomolecules, but also endows additional functions derived from NCPs [26–29].

Herein, we would like to summarize the most recent advances in several biomolecule-based NCPs composites. It should be noted that most NCPs discussed in this work are mainly crystalline porous materials. Approaches in the construction of different types of guest molecules, like amino acids, nucleic acids, enzymes and lipids are introduced respectively. More importantly, the relevant applications in the areas of sensing, catalysis, molecular imaging and drug/gene delivery and therapy are also illustrated in detail (Fig. 1). Finally, current challenges and prospective are discussed. In this review, we intend to provide a systematic overview about the engineering and applications of NCPs with biomolecules, which may provide helpful guidance and hints for future investigations.

2. Integration of biomolecules with NCPs

In general, several approaches have been developed for the integration of biomolecules with NCPs: 1) biomolecules can directly work as the building units to obtain NCPs; 2) biomolecules can diffuse into the pores or be attached on the surface of NCPs *via* physical interactions; 3) some biomolecules containing functional groups can be covalently conjugated with NCPs; and 4) biomolecules can also be directly immobilized into NCPs matrix through *in situ* encapsulation. In this section, strategies towards different types of biomolecule-NCP composites will be described in detail. Pros and cons of each approach will also be evaluated for future directions in the design of biomolecule-based NCPs composites.

2.1. Amino acids or peptide-based composites

Amino acids are basic small biomolecules, along with the amine (–NH_2) and carboxyl (–COOH) groups attached to the first carbon atom, while peptides are short chains of amino acids linked by amide bonds. Amino acids or peptides can be directly used as organic linkers for NCPs synthesis. Also, they can be loaded into the pores or covalently modified on the surface of the NCPs.
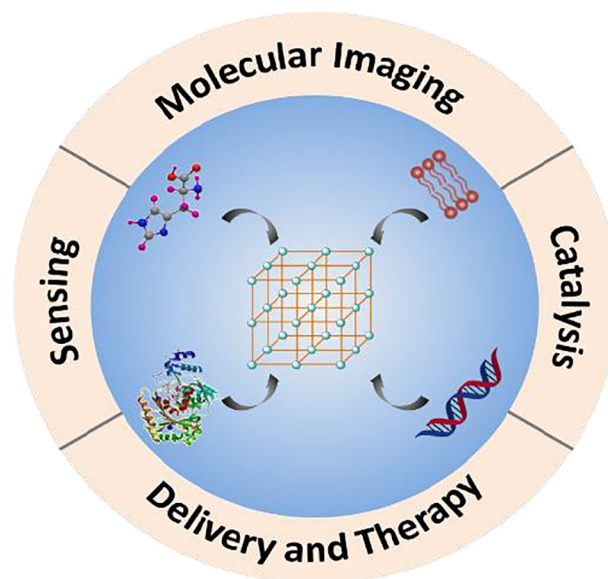

Fig. 1. Schematic illustration of NCP-biomolecule composites for advanced applications.

2.1.1. Amino acids or peptides as the building ligands

Due to the presence of the carboxyl and amino groups in the structure, amino acids and peptide could coordinate with metal ions *via* the O, N-chelation mode. Usually, the pure amino acids could be used to construct the one-dimensional network, whilst extended MOF structures with two- or three-dimensions could be created *via* bi- or tri-dentate bridging modes [30]. For example, the coordination between glycine and Ni, Mn or Co could construct two-dimensional metal-ion amino acid frameworks. Also, bi-dentate bridging mode could be constructed between L-phenylalanine (Phe) or L-glutamine (Gln) with Cu. In addition, some reactive side chains of amino acids, like the imidazole group of histidine (His), the phenol group of tyrosine or the thiol group of cysteine could provide additional binding sites to metal ions [31].
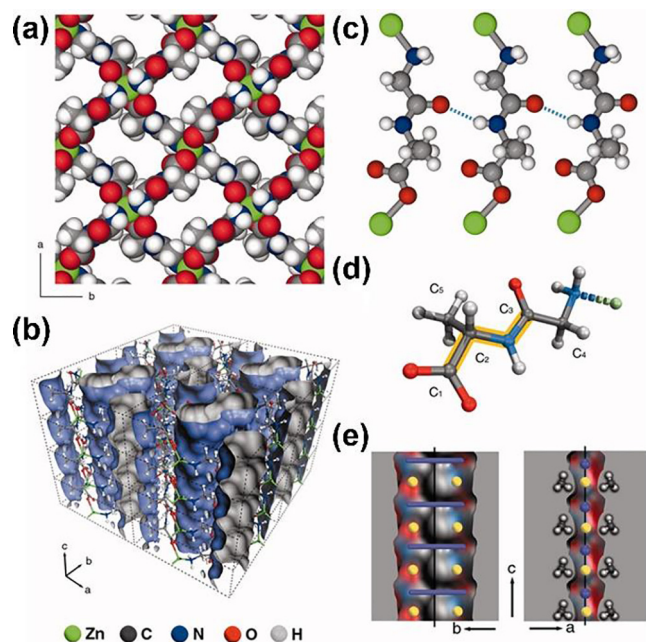
More detailed discussions about using the amino acids as linkers to construct different dimensional frameworks could be found elsewhere [24].

Compared to single amino acids, peptides that combine different types of amino acids together enable more diverse and flexible poly-dentate bridging modes for the construction of bio-MOFs. The pioneering works on dipeptide-based MOFs were reported by Ros-seinsky group [32–35]. They adopted Zn to coordinate with several dipeptides to afford a range of frameworks with distinct performances. For example, the metal-dipeptide framework [Zn(Gly-Ala)$_2$]·(solvent) was reported with the adaptable porosity, which could transit from the closed to open-pore forms in response to small polar molecules (Fig. 2) [32]. Compared to [Zn(Gly-Ala)$_2$], the structure of Zn(Gly-Thr)$_2$ is more rigid due to the additional hydrogen-bonding interactions [33]. Later, a special natural dipep-tide carnosine (β-alanyl-L-histidine) was adopted to construct a porous 3D framework. The imidazole group in the histidine resi-dues endows more metal binding sites, affording better chemical stability, permanent microporosity and chirality [34]. Besides dipeptides, tripeptide Gly-His-Gly (GHG) was also explored as the backbone to construct Cu(II)-based 3D MOF for enantioselec-tive separation of chiral drugs [35].

To sum up, by modulating amino acids or peptide sequences, the conformation and dimension of frameworks will change accordingly, which will finally influence the flexibility, stability and affinity for guest molecules. However, a limited number of amino acid- or peptide-based frameworks have been well-studied with regard to the potential versatility of constituent peptides.

2.1.2. Amino acids or peptides encapsulation

In an early attempt to integrate peptides with MOFs, Matsui *et al.* developed a smart autonomous motor consisting of the por-ous MOF as the storage cell and diphenylalanine (DPA) peptide as the guest molecule [36]. The MOF could be partially degraded by sodium ethylenediaminetetraacetate (Na-EDTA) to release the DPA peptides, followed by the self-assembly of DPAs at the water/MOF interface. Then the reorganization of peptides could create large surface-tension gradient around MOF, leading to the effective swimming motion. Due to the controlled movement in the direction of the higher surface tension side, they applied this DPA-MOF system for sensing potential chemical targets in their follow-up work [37]. The designed peptide would swim towards higher pH area where the DPA presented increased solubility (Fig. 3a).

Fig. 2. The structure and perspective view of Zn(Gly-Ala)$_2$. (a) Space-filling representation viewed along the *c* axis. (b) Perspective view of channels in Zn (Gly-Ala)$_2$. (c) The interlayer hydrogen-bonding interactions. (d)The view of Gly-Ala dipeptide ligand. (e) Cross sections of a pore Connolly surface. Reprinted with permission from Ref. [32]. Copyright 2010, American Association for the Advance-ment of Science.
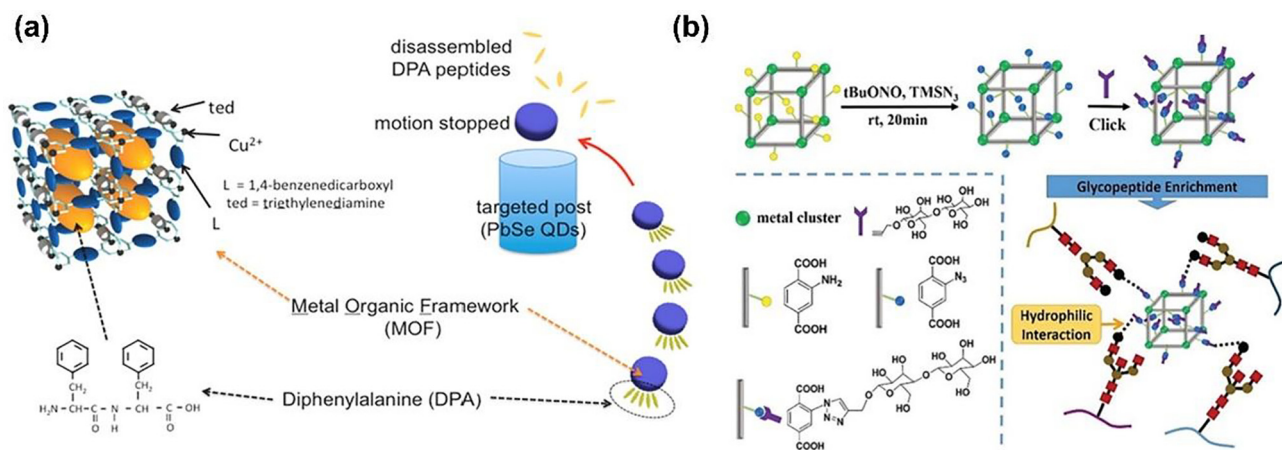

Fig. 3. (a) Schematic of peptide-MOFs swimmers to direct the motion of hydrophobic DPA peptides towards high pH area. Reprinted with permission from Ref. [37]. Copyright 2015, American Chemical Society. (b) The synthesis of MIL-101(Cr)-maltose. Reprinted with permission from Ref. [38]. Copyright 2016, Royal Society of Chemistry.

Besides the small peptide encapsulation, MOFs have also been used for the enrichment of glycopeptide with the higher molecular weight. Liu and co-workers reported maltose-functionalized MOFs MIL-101(Cr)-maltose through two-step modification (Fig. 3b). The synthesized MIL-101(Cr)-NH$_2$ which firstly can react with azidotrimethylsilane (TMSN$_3$) and *tert*-butyl nitrate (tBuONO) to obtain the azide-functionalized MIL-101(Cr)-N$_3$. Then MIL-101 (Cr)-maltose could be obtained by the subsequent click reaction with 1-propargyl-O-maltose. The characteristics of MOFs and hydrophilic maltose groups can greatly facilitate the glycopeptide enrichment, leading to highly sensitive and efficient glycoproteomic analysis in the human serum sample [38].

2.1.3. Post-synthetic modification

Besides the incorporation of peptides as the linkers or payloads, MOF can also be modified *via* the post-synthetic pathway. Through covalent coupling reactions, peptide could be conjugated with the organic linkers in the preformed MOF. The common approach to peptide conjugation is the amide reactions between carboxylic acid and amine under the mild condition by using the coupling reagent. Wuttke and coworkers tried to figure out the optimal coupling conditions by comparing four different coupling reagents (Fig. 4a) [39]. They utilized amino-functionalized MIL-101(Al)–NH$_2$ to react with acetic acid by employing diisopropylcarbodiimide(DIC), 1,10-carbonyldiimidazole (CDI), N,N,N0,N0-tetramethyl-O-(1H-benzotriazol-1-yl)uronium hexafluorophosphate (HBTU) or bromotripyrrolidinophosphonium hexafluorophosphate (PyBroP) as the coupling reagents. The results indicated that DIC achieved the best coupling efficiency.

Jonathan and coworkers developed an example of microwave-assisted postsynthetic modification method on grafting peptides inside the MOF cavities (Fig. 4b) [40]. The MOFs with different topology, dimensionality and pore sizes were applied to investigate the methodology. The results showed that the microwave irradiation could effectively improve the coupling yield without peptide racemization. Later, Yaghi and coworkers carried out the microwave-assisted reactions by covalently attaching tripeptide (H$_2$N-Pro-Gly-Ala-CONHL and H$_2$N-Cys-His-Asp-CONHL, with Gly = glycine, Pro = proline, Asp = aspartic acid, His = histidine, Cys = cysteine, and L = organic struts) to amino-functionalized (-CH$_2$NHBoc) MOF [41]. The properly designed multivariate MOF

complex exhibited enzyme-like properties to proceed catalytic reactions (chlorinations or peptide cleavage).

2.2. Nucleic acids-based composites

As the well-known fundamental biomolecules, nucleic acids are ubiquitously present in all animals and plant cells. Depending on the difference of sugar moiety, nucleic acids are divided into deoxyribonucleic acid (DNA) and ribonucleic acid (RNA), which play critical roles in the storage and transmission of genetic information and protein synthesis. The key constituents, nucleobases with the amine or imine groups allow them to act as favored building linkers to form the finite or infinite molecular assemblies with metals [42]. The structure could be constructed *via* the coordination chemistry (π-π stacking, electrostatic interactions, and H-bonding) or covalent conjugation.

2.2.1. Nucleobases as the building ligands

Like amino acids or peptides as building units, nucleobases are also widely applied to construct metal–organic coordination polymers due to their several accessible oxygen and nitrogen donor sites. The multiple interactions and binding modes between the nucleobases and metal ions facilitate the formation of bio-MOFs and some biologically active metallodrugs. Additionally, nucleobases are abundant in nature and environmentally friendly, which makes them good candidates for the design of bio-MOFs. Among the nucleobases, adenine is the most widely explored molecule for the construction of porous materials, given its rich coordination modes with four N atoms and one amino group in the rings [24,43,44].

The Rosi group reported a representative example of adenine-incorporated single crystalline material bio-MOF-1 (Fig. 5a), formulated as Zn$_8$(ad)$_4$(BPDC)$_6$·2Me$_2$NH$_2$·8DMF·11H$_2$O [44]. They further explored the anionic properties for the storage and release of cationic drug molecules. Later, the same group obtained a new type of mesoporous material bio-MOF-100 (Fig. 5b) with zinc-adeninate octahedral building units as discrete vertices, formulated as Zn$_8$(ad)$_4$(BPDC)$_6$O$_2$·4Me$_2$NH$_2$·49DMF·31H$_2$O [45]. Compared to the previous Bio-MOF-1, bio-MOF-100 exhibited higher surface area (4300 m^2 g^{-1}) and larger pore volume (4.3 cm^3 g^{-1}). Despite the benefits of nucleobase, the lack of symmetry of
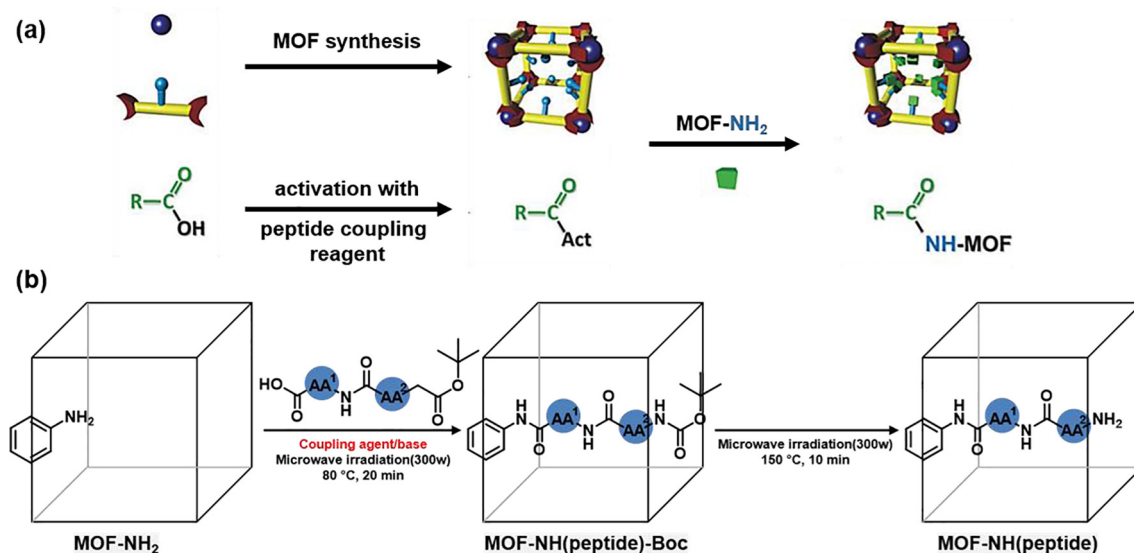

Fig. 4. (a) Schematic of postsynthetic modification of amino-MOF *via* coupling reactions. Reprinted with permission from Ref. [39]. Copyright 2014, Royal Society of Chemistry. (b) Microwave assisted modification of peptide into MOFs. Reprinted with permission from Ref. [40]. Copyright 2015, American Chemical Society.
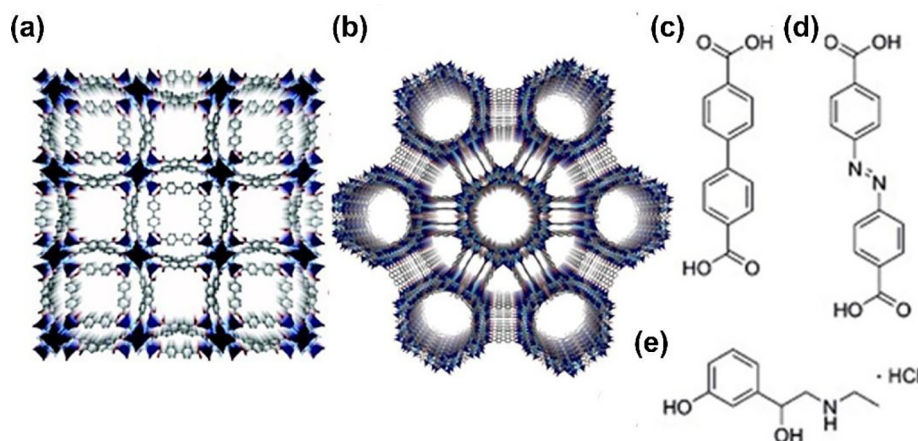
Fig. 5. The crystal structure of bio-MOF-1 (a) and bio-MOF-100 (b). Reprinted with permission from Ref. [44]. (c) BPDC, (d) Azo-BPDC, and (e) etilefrine hydrochloride. Copyright 2009, American Chemical Society. Reprinted with permission from Ref. [45]. Copyright 2012, Nature Publishing Group.

nucleobases and no control of binding modes may impede their formation of bio-MOFs. To overcome the low-symmetry nature of adenine, Zhou group introduced a highly symmetric co-ligand to obtain a new type of metal organic materials PCN-530, formulated as $Zn_3[Zn_2(\mu_2-H_2O)]_3(Ad)_6(TATB)_4(DMF)$, (Ad = adeninate, TATB = 4,4′,4″-s-triazine-2,4,6-triyl-tribenzoate) [46]. Besides adenine, another blocky crystal of TMOP-1 (thymine-incorporated metal–organic polyhedron), formulated as $Cu_{24}(MDPI)_{24}(DMA)_4(-H_2O)_{20}$ (MDPI = 5-((5-methyl-2,4-dioxo-3,4-dihydropyrimidin-1(2H)-yl)methyl)isophthalate), was also obtained *via* direct reactions between copper acetate and H_2MDPI [46].

Very recently, Li group developed DNA-based nanoparticles *via* the coordination-driven self-assembly approach [47]. The one-pot reaction between DNA molecules and Fe^{II} ions at 95 °C enabled the formation of monodisperse spherical nanoparticles with the average size distribution of 191 ± 30 nm. Further detailed mechanism studies revealed that the assembly process was DNA sequence-dependent and nucleotide coordination affinity to Fe ions was in the order of A > G > C > T. Finally, the as-prepared Fe-CpGs nanoparticles exhibited relatively high DNA delivery and antitumor efficacy both *in vitro* and *in vivo*.

2.2.2. Oligonucleotide conjugation

Another feasible approach for fabricating nucleic acid-based NCP composites is to covalently conjugate the oligonucleotide with the well-prepared coordination polymers. The Mirkin group reported an example of nucleic acid-MOF nanoparticle conjugates through the covalent coupling strategy [48]. They synthesized the azide-functionalized zirconium-based framework, UiO-66-N$_3$, followed by the conjugation with dibenzocyclooctyne (DBCO)-modified DNA *via* the Cu-free click chemistry. The DNA modification on the surface offered the steric and electrostatic barriers to aggregation, resulting in the increased colloidal stability in high dielectric media when compared to the unfunctionalized MOFs. Moreover, the *in vitro* studies revealed that the DNA-MOF constructs had better cellular internalization, as compared to free DNA or naked MOF nanoparticles (Fig. 6a).

Another example reported by Kahn *et al.* described the development of pH- and K^+-ion-responsive DNA-functionalized MOFs for switchable release of payloads [49]. The well-established MOFs were modified with DNA *via* EDC/NHS based amide coupling reactions (Fig. 6b). Three different DNA switching motifs were involved to achieve the controlled unlock of the DNA gates, followed by the stimulated release of fluorescent molecules. Recently, He and coworkers developed the DNA-assembled core-satellite nanoparti-

cle superstructures, which are composed of the PCN-224 MOF and upconversion nanoparticles (UCNPs) [50]. Both MOFs and UCNPs expose NH_2 groups on the surface, which can react with the linker dibenzocyclooctyne N-hydroxysuccinimidyl ester (NHS-DBCO), followed by the conjugation of two complementary azide-modified DNA strands respectively. The DNA-mediated hybridization allowed the formation of the MOF-UCNP core-satellite super-structures for improved photodynamic therapy under NIR light irradiation (Fig. 6c).

In addition to covalent conjugation on the surface of MOFs, DNA sequences can also coordinate with the unsaturated metal ion sites directly. The Mirkin group applied the terminal phosphate-modified oligonucleotides to coordinate with unsaturated metal sites on the MOF surface (Fig. 6d) [51]. To develop a general strategy, nine kinds of distinct MOF particles were successfully functionalized with oligonucleotides with tunable properties for different purposes. By employing the similar strategy, nucleic-acid modified NU-1000 and PCN-222 NPs were synthesized to load insulin protein [52]. It was found that the oligonucleotide-rich surfaces of MOFs enabled 10-fold increase of cellular uptake. Overall, this approach is independent of the structure of organic ligands and could be applied to prepare a broad class of NCPs.

2.2.3. Oligonucleotide encapsulation

Due to their negative charge property, oligonucleotides can be readily absorbed or encapsulated into the NCPs to form the composites, which are often used for nucleic acid detection or gene delivery. The two-dimensional sheet of N,N-bis(2-hydroxy-ethyl) dithiooxamidatocopper(II) (H_2dtoaCu) MOF is a well-established example of DNA/RNA sensing platform [53–56]. Because of the existence of Cu^{2+} metal center and π-stacking effect, this nanosheet not only can effectively absorb the fluorescently labeled oligonucleotides *via* hydrophobic interactions, but also quench the signals through the photoinduced electron transfer (PET) effect. The presence of target DNA/RNA would facilitate the recovery of fluorescence. Similarly, the UiO-66 was also applied for the sensing of miRNA reported by Kang group [57].

Besides the DNA/RNA sensing, the encapsulation into MOF materials could also help control the stability of trapped oligonucleotides. Xia group reported the self-assembly of three-dimensional DNA tetrahedral nanostructure and M_6L_4 sphere framework *via* electrostatic and hydrophobic interactions [58]. The newly formed composite greatly improved the stability of DNA in water and maintained its genetic information. Lin group developed the UiO MOFs to co-deliver cisplatin prodrug and
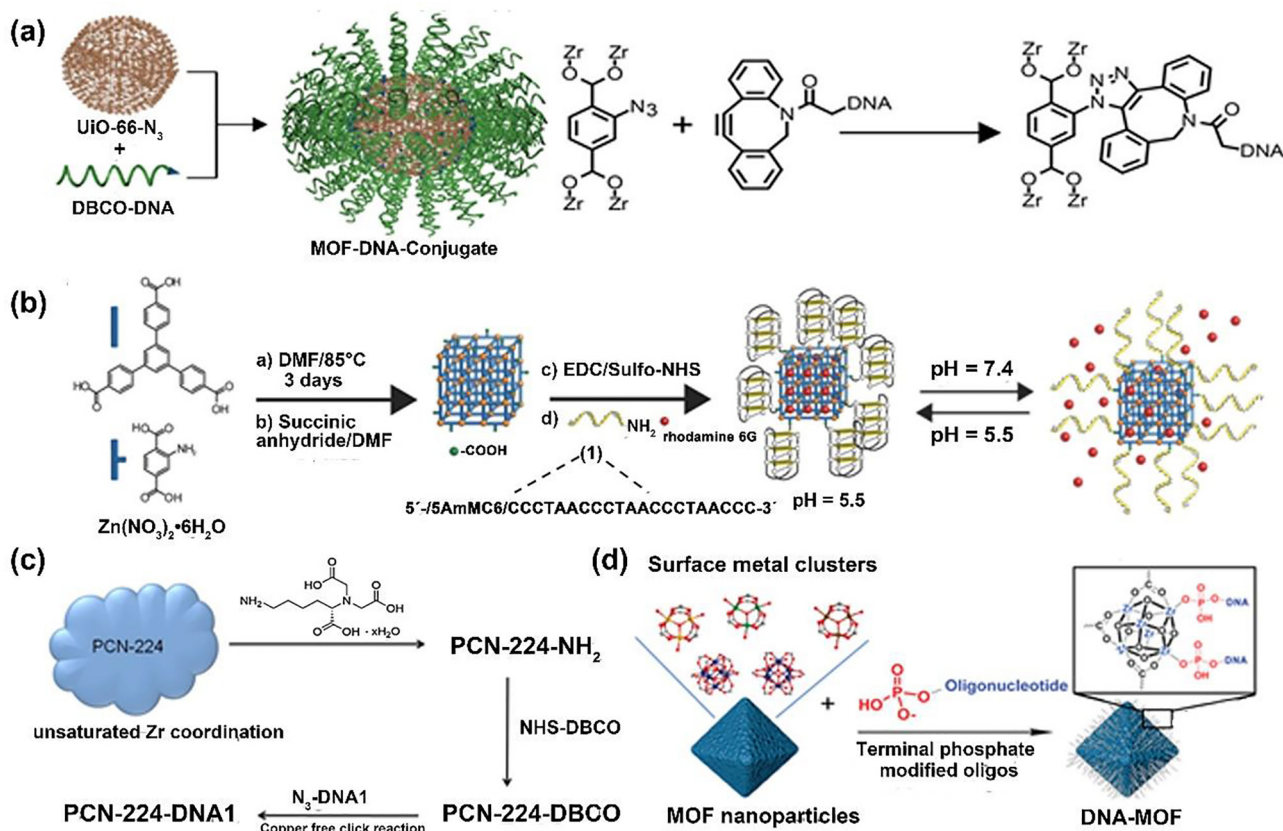
Fig. 6. Schematic illustration of DNA-functionalized MOFs. (a) Synthesis of UiO-66-N$_3$ by copper-free click reaction between nano-MOF and DBCO-DNA. Reprinted with permission from Ref. [48]. Copyright 2014, American Chemical Society. (b) Synthesis of i-motif functionalized MOFs for pH-responsive dye release. Ref. [49]. Copyright 2017, Wiley-CH. (c) Synthesis of DNA-modified PCN-224 NPs. Ref. [50]. Copyright 2017, Royal Society of Chemistry (d) Synthesis of DNA-MOF using terminal phosphate-modified oligonucleotides. Ref. [51]. Copyright 2017, American Chemical Society.

siRNAs into ovarian cancer cells [59]. Compared to the covalent conjugation, physical encapsulation is more applicable for widespread use due to its easy operation, while the size of oligonucleotides should be carefully considered before their loading into the pore size of NCPs.

Very recently, Zhou and Deng group achieved the precise inclusion of single-stranded DNA (ssDNA, 11–53 nt) into MOFs through the precise control of pore size [60]. They synthesized a series of MOFs (NiIRMOF-74-II to -V) with varying pore size to investigate the reversible interactions between MOFs and ssDNA (Fig. 7). The detailed studies on the uptake, protection and release of ssDNA revealed that all MOFs could include the ssDNA into the pores and protect the payload from degradation, while Ni-IRMOF-74-II showed the best release performance (55.0% release of the loaded ssDNA) over other Ni-IRMOF-74 series. Subsequently, they applied these MOFs as vectors for the intracellular delivery and gene silencing. Results suggested that Ni-IRMOF-74-II and -III with weaker interactions presented the optimal transfection efficiency in mammalian immune cells over other materials.

2.3. Enzyme-based composites

As one intriguing and important class of natural macromolecules, enzymes have received great attention due to their roles in catalyzing more than 5000 biochemical reaction types [61]. As the biological catalysts, enzymes play critical roles in cell regulation and signal transduction. They are also found to have high relevance with the progression of numerous diseases like inflammation, osteoarthritis, neurodegeneration and cancer, etc.

[62]. Due to the great merits in the catalytic specificity, high affinity for the substrate and green chemistry, enzymes have been increasingly utilized in the health care, chemical industry and other related areas [63]. However, their undesired instability in harsh conditions, low tolerance to pH values, short shelf-storage life and difficulties in recycling severely restricted their widespread applications [64]. Hence, immobilizing enzymes on solid supports may become a promising solution to overcome these issues [65]. In this section, current methods for enzyme immobilization in NCPs will be provided and typical examples for the enzyme-based composites will be discussed in detail.

2.3.1. Physical absorption

Like other biomolecules, enzymes can be either physically attached on the surface or loaded into the cavity of NCPs. The surface attachment through nonspecific interactions between NCPs and enzymes is a relatively straightforward approach, which has no requirement on the pore size or any functional groups. Balkus and coworkers made an early attempt to investigate hybrid materials for physical immobilization of microperoxidase-11(MP-11) catalyst [66]. Five different mesoporous benzene silica (MBS) materials and Cu-MOFs as the host materials were evaluated accordingly. Results implied that the Cu-MOF supported MP-11 showed better enzymatic activity. Similarly, Mao and Yang group explored a series of zeolitic imidazolate frameworks (ZIFs) with different pore sizes, surface areas and functional groups to co-immobilize methylene green (MG) and glucose dehydrogenase (GDH) [67]. ZIF-70 was found to exhibit best performance as the matrix and the prepared ZIF-70-based electrochemical biosensor
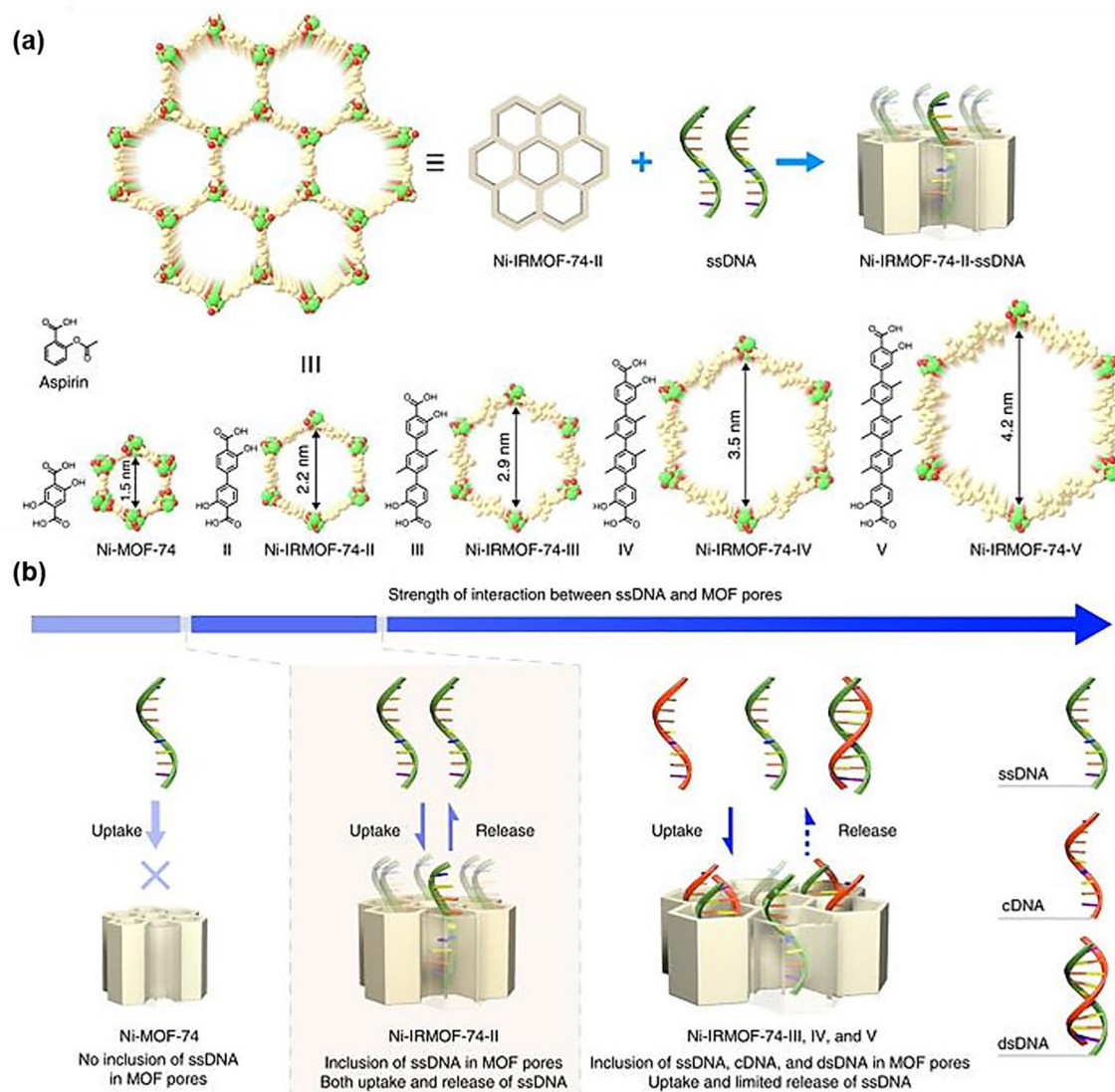
Fig. 7. (a) Schematic illustration of the encapsulation of ssDNA into MOFs *via* tuning the pore size of MOFs. (b) The uptake and release process of ssDNA. Reprinted with permission from Ref. [60]. Copyright 2018, Nature Publishing Group.

enabled real-time monitoring of glucose in the brain of guinea pigs (Fig. 8a).

Besides the surface attachment, enzymes can also be absorbed into the pores of the NCPs. A series of pioneering studies on the encapsulation of various enzymes were reported by Ma group. In an early study, they first incorporated the MP-11 with dimensions of about $3.3 \times 1.7 \times 1.1$ nm into a mesoporous Tb-TATB MOF [68]. The Tb-TATB (hereafter denoted Tb-mesoMOF) with nanoscopic cages of 3.9 and 4.7 nm in diameter was utilized to mix with MP-11, leading to the formation of denoted MP-11@Tb-mesoMOF. The mesoporous MOF host matrix could greatly stabilize this catalyst and preserve its catalytic performances, compared with the mesoporous silica materials as the carrier. Later, they also successfully loaded the myoglobin (Mb) with relatively larger size into mesoporous MOF with hierarchical pore sizes [69]. The possible reason for the successful immobilization is attributed to the dynamic and flexible structure of Mb molecules. However, the small pore size of $\sim$0.8 nm in MOF structure only allowed small substrate molecules to get access to the enzyme site, resulting in its size-selective biocatalysis. The following study revealed that Cyt c had to undergo the conformational changes before they were able to enter the interior of MOF (Fig. 8b) [70].

In addition to the relatively small pored MOFs, ultra-large mesoporous cages were also developed by Zhou group for enzyme engineering (Fig. 8c) [71]. PCN-333 with a cage size of 5.5 nm was able to encapsulate three enzymes, horseradish peroxidase (HRP), Cyt c and MP-11. The custom-designed platform exhibited high loading capability, where the HRP and Cyt c underwent single-enzyme encapsulation (SEE) and MP-11 went through multiple-enzyme encapsulation (MEE), respectively. The enzymatic kinetics data demonstrated smaller K_m values of immobilized enzymes when compared to the free enzymes, suggesting higher affinity for the substrate. Moreover, such rationally designed composites are more advantageous in minimizing enzyme aggregation and leaching, favored recyclability and better performances in harsh organic conditions. However, such method is limited to the pore size of the host matrix. Only a few examples are developed for successful loading of enzymes. Therefore, it is very necessary to explore more efficient approaches for enzyme immobilization.

2.3.2. Covalent conjugation

Due to the presence of free amino or thiol groups, a facile way to immobilize the enzymes within NCPs is covalent conjugation [72–74]. Jung *et al.* firstly established coordination polymers or MOFs
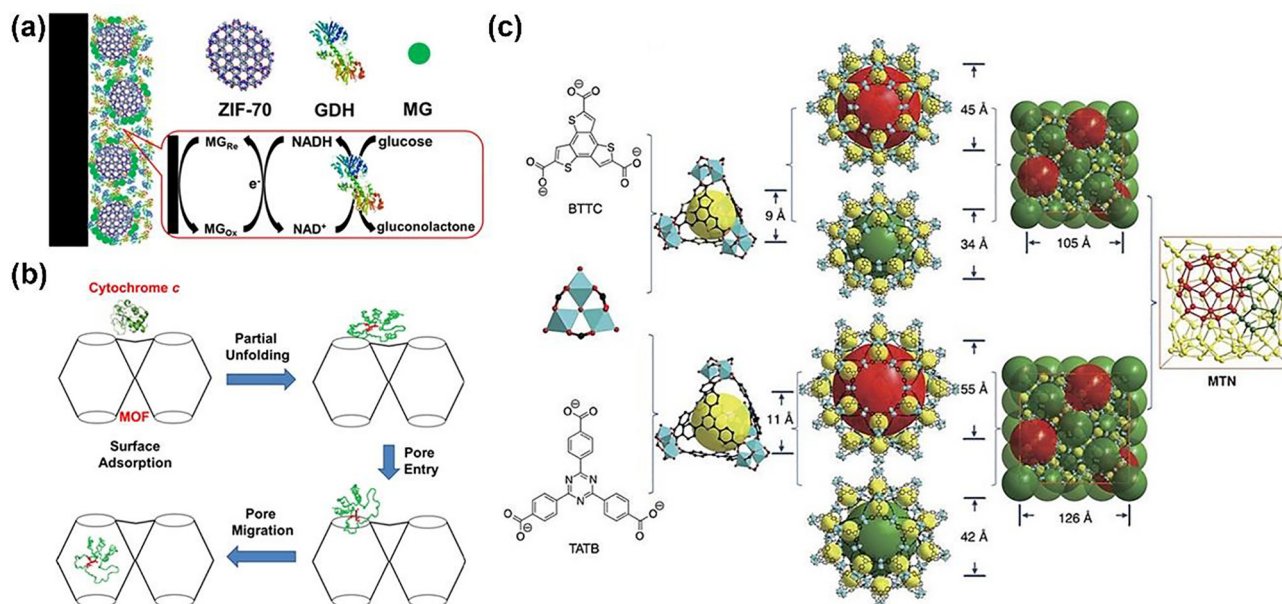
Fig. 8. (a) Schematic illustration of ZIF-70 based electrochemical biosensor by co-immobilization of MG and GDH. Reprinted with permission from Ref. [67]. Copyright 2013, American Chemical Society. (b) The mechanism of Cyt c incorporation into MOF cavities *via* partial unfolding [70]. Copyright 2013, American Chemical Society. (c) Schematic illustration of ligands and cages in PCN-332 and PCN-333. Reprinted with permission from Ref. [71]. Copyright 2015, Nature Publishing Group.

attached with enhanced green fluorescent protein (eGFP) and Candida-antarctica-lipase-B (CAL-B) enzyme [72]. The dangling carboxylate groups on the surface of MOFs were activated by the coupling regents such as (3-dimethylaminopropyl) carbodiimide (EDC) or dicyclohexyl carbodiimide (DCC), followed by the protein conjugation step. Then they assessed the catalytic activity of CAL-B-MOF conjugates in the transesterification of (±)-1-phenylethanol. The results indicated that CAL-B coated coordination polymers not only maintained the enantioselectivity, but also presented up to three orders of magnitude higher activity than the native enzyme. Although not verified, the proposed reason for

higher activity is probably derived from more efficient enzyme-substrate contact due to the confined space provided by MOFs.

Shin *et al.* reported trypsin-immobilized MOF reactors by using the similar coupling method [73]. As depicted in Fig. 9, three chromium based MOFs: MIL-88B ($[Cr_3F(H_2O)_2O(bdc)_3]$), MIL-88B-NH$_2$ ($[Cr_3F(H_2O)_2O(NH_2\text{-}bdc)_3]$) and MIL-101 were selected and activated by DCC, followed by the nucleophilic attack of the amine groups of trypsin. Subsequently, these trypsin-MOF reactors were applied to digest BSA protein with 2 min of ultrasonication. The nanoLC-MS^2 chromatography indicated similar MS signal intensities and the number of matched peptides from
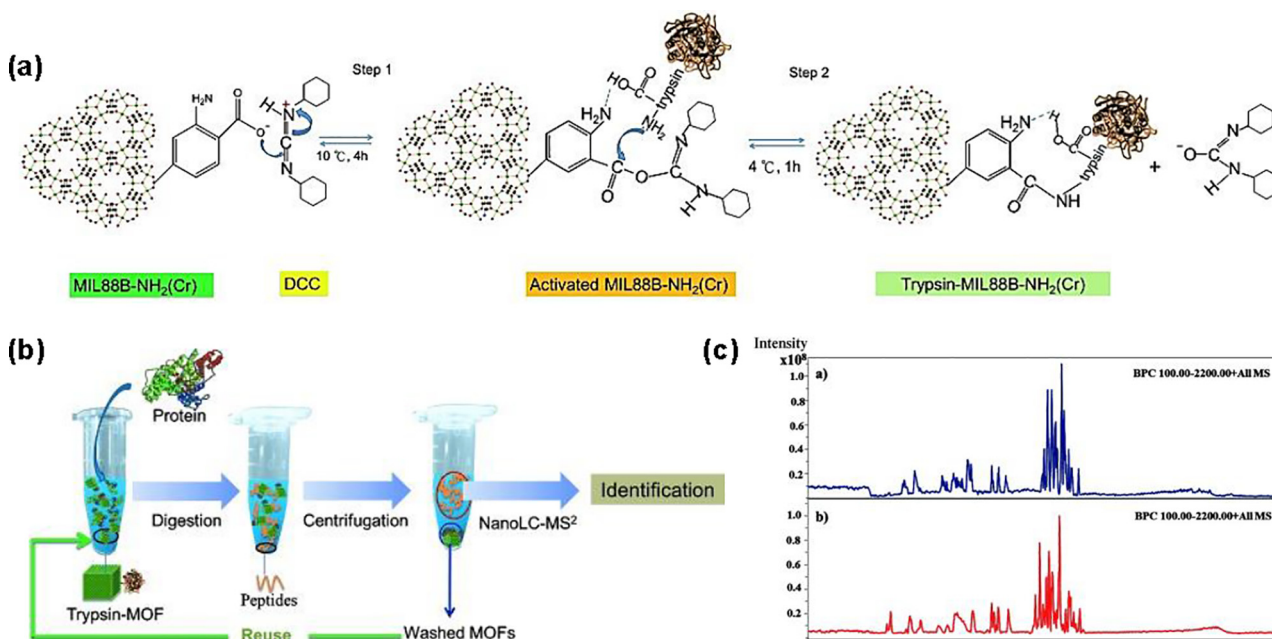

Fig. 9. Schematic of trypsin conjugation with MIL-88B and protein digestion by trypsin-MOF. Reprinted with permission from Ref. [73]. Copyright 2012, Wiley-VCH.
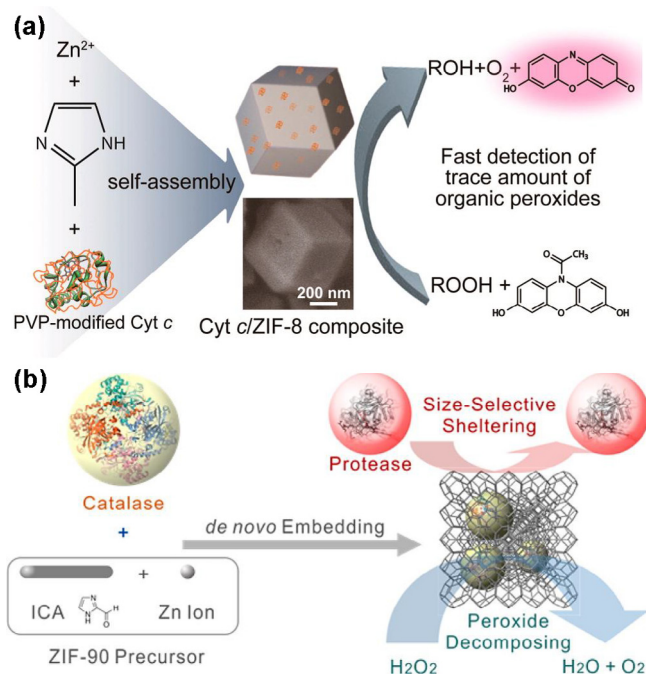
Fig.10. (a) Synthesis of Cyt c-embedded ZIF-8 and catalytic reaction on the detection of organic peroxides. (b) Synthesis of catalase-ZIF-90 composite and its functional activity Reprinted with permission from Ref. [75,76]. American Chemical Society.

trypsin-MIL-88B-NH$_2$(Cr) reactors as compared to native trypsin digestion. Detailed investigations revealed that the amino groups of MOFs could facilitate the trypsin immobilization and BSA digestion through the hydrogen bonding interactions. In short, the great reusability, stability and digestion efficiency resulted in the improved overall performance compared to free enzyme.

2.3.3. De novo method

The *de novo* approach, in which enzymes could be directly embedded into the NPs during the process of nanoparticle formation. The *de novo* method could effectively encapsulate enzymes with larger size regardless of the pore size. Liu group proposed a facile synthetic method to embed Cyt c into the zeolitic imidazolate framework (ZIF-8) [75]. Initially, the Cyt c was modified with polyvinylpyrrolidone (PVP), which acted as the additive to assist the dispersion of Cyt c in methanol. Then the formed complex solution was added into the solution of zinc nitrate hydrate and 2-methylimidazole to obtain Cyt c/ZIF-8 composite (Fig. 10a). Further investigations revealed that the Cyt c molecules were mainly localized on the crystal surface, where their native configuration was well maintained. The Cyt c embedded in ZIF-8 had about 10-fold higher peroxidase activity for sensitive detection of the explosive organic peroxides in the solution.

Similar *de novo* approach was employed by Shieh *et al.* to obtain CAT@ZIF-90 composite under aqueous condition (Fig. 10b) [76]. They chose the ZIF-90 with smaller pore size of ~1 nm to immobilize catalase molecules with large size of ~10 nm for the purpose of size-selective sheltering function and prevention from the leakage. Different from the Cyt c/ZIF-8 composite, the catalase molecules were verified to be embedded inside the ZIF-90 crystals, rather than on the external surface. However, the enzymatic activity of catalase was preserved well, even in the presence of proteinase K, which will cause the loss of activity of pure catalase.

In addition to the enzyme encapsulation, Liang *et al.* expanded such similar method to embed a variety of biomolecules including proteins, DNA and enzymes into a class of porous MOF materials [77]. The morphology and crystal size could be rationally controlled *via* the biomimetic mineralization process. Moreover, the payloads could be released from the protective frameworks in response to pH changes, enabling the potential use in the area of biobanking or drug delivery.

So far, only a few types of NCPs, like ZIF-8, ZIF-90 (linker: 2-imidazolate carboxaldehyde), and MAF-7 (linker: 3-methyl-1,2,4-triazolate) are adaptable for the encapsulation of biomolecules through the *de novo* method [78–82]. The main reason is the preparation process in the presence of biomolecules requires the biocompatible synthetic conditions, which may hinder the formation of most NCPs. Hence, the discovery of more NCPs with mild synthetic routes is highly demanded in order to expand the widespread use of this strategy. Apart from this, the structure and activity of proteins or enzymes when encapsulated on the surface or inside the NCPs should be carefully investigated. Proteins or enzymes are readily proximity to the hydrophobic surface of materials, which may alter their orientation, leading to the loss of activity. So recent findings proposed that hydrophilic materials may help retain the original enzymatic activities [82]. In short, surface properties of NCPs matrix may have a substantial effect on the enzymatic behaviors, which may need to be further explored when applied for the effective biomolecule protection.

2.4. Lipid-based composites

As one family of amphiphilic molecules, lipids are broadly distributed in nature, like fatty acids, waxes, sterols, vitamins, *etc*. In terms of various biological functions of lipids, the well-known fact is that lipids are the indispensable structure components of cell membranes. Due to the amphiphilic nature of lipids, they are easily formed into vesicles, which are widely utilized to improve solubility or stability of various nanomaterials. Lin group did several investigations on lipid coated NCPs [83–85]. In one typical study, they synthesized the Zn(II) bisphosphonate NCPs with the cisplatin prodrug in the presence 1,2-dioleoyl-*sn*-glycero-3-phosphate sodium salt (DOPA) through the reverse microemulsion method (Fig. 11a). The NCPs were further coated by the mixture of 2-dioleoyl-snglycero-3-phosphocholine (DOPC), cholesterol and 1,2-distearoyl-*sn*-glycero-3-phosphoethanolamine-N-[methoxy(polyethylene glycol)-2000] (DSPE-PEG$_{2k}$) in a 4:4:2 M ratio, resulting in the formation of lipid bilayer on the surface. The assembled NCPs exhibited prolonged circulation time and enhanced drug deposition at tumor sites [84].

Similarly, Bein and coworkers modified the MIL-100(Fe) and MIL-101(Cr) nanoparticles with lipid DOPC through solvent-exchange deposition method (Fig. 11b) [86]. The lipid initially existed in the monomer form in EtOH/H$_2$O mixture, while lipid bilayer could gradually form on the nanoparticle surface as the water concentration increased. The results demonstrated that MOF@lipid system could effectively prevent the dye release from the pores. Moreover, cell studies indicated that the efficient uptake could facilitate the next-step imaging and drug delivery.

3. Applications of biomolecules-NCPs composites

Due to the porous structure, tunable metal centers and organic linkers of NCPs, the integration of biomolecules and NCPs have shown great potentials in various areas. In this section, we provide the most recent progress on biomolecules-NCPs composites in the application of sensing, catalysis, molecular imaging and delivery and delivery and therapy.
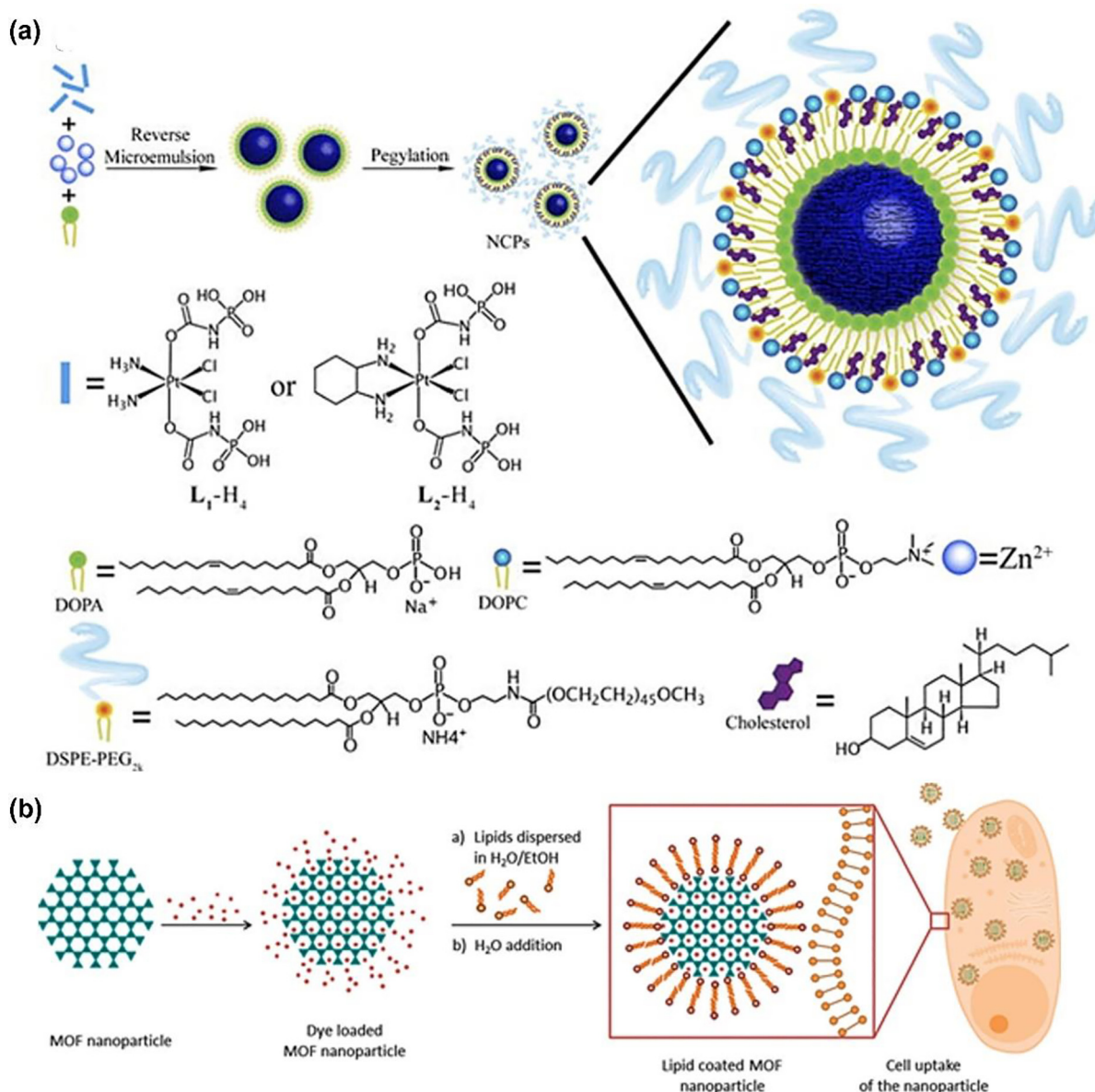
Fig.11. (a) Schematic illustration of lipid-coated NCPs. Reprinted with permission from Ref. [84]. Copyright 2015, Nature Publishing Group. (b) Synthesis of dye-loaded MOFs and further coating with lipid. Reprinted with permission from Ref. [86]. Copyright 2017,Royal Society of Chemistry.

3.1. Sensing

Because of versatile approaches to immobilization of biomolecules on NCPs, numerous proteins and nucleic acids with different recognition functionalities have been developed as NCP-based sensors for the detection of biologically or environmentally significant molecules, such as glucose, hydrogen peroxide (H_2O_2), DNA, and so on [75,87–89]. Compared to the biomolecules alone, these hybrid materials offer much better performances in several aspects, such as sensitivity, stability and selectivity. More comprehensive reviews about the NCP or MOF-based sensing applications have been reported elsewhere [7,90].

Hou *et al.* reported the glucose oxidase (GOx) embedded magnetic zeolitic imidazolate framework 8 (mZIF-8@GOx) *via* the *de novo* approach for fast detection of glucose [87]. Glucose could be oxidized to generate H_2O_2, which will continuously oxidize o-phenylenediamine (OPD) to obtain the orange-color product. Results indicated that the composite exhibited not only higher operational stability at high temperature and wider pH conditions compared to native GOx, but also higher sensitivity and selectivity

to glucose with the limit of detection (LOD) of 1.9 μM. Moreover, magnetic properties of mZIF-8 endowed their favored recyclability. As discussed in Section 2.3.3, the Cyt c/ZIF-8 composite was established to detect H_2O_2 or explosive organic peroxides in the solution [75]. The detection limit for H_2O_2 is 3 nM with good liner range of 5 nM–1 μM. Similarly, Yang and coworkers developed one-pot synthesis of the bovine hemoglobin (BHb)-embedded ZIF-8 hybrid composite, which displayed over 4 times increase of catalytic activity compared to free BHb [88]. Then it was successfully applied as a colorimetric sensing platform for the detection of H_2O_2 and phenol with the detection limit up to 1 μM for each analyte. Apart from this, MOF-encapsulated enzymes have been used to fabricate electrochemical biosensors. Chen *et al.* designed a HRP@PCN-333(Fe)-based biosensor with improved acid and thermal stabilities for the detection of H_2O_2 [91]. Such enzyme-MOF biosensor system exhibited excellent analytical performance with a low detection limit of 0.09 μM.

For the MOF-based sensing, DNA and RNA are always favored targets. The construction of nucleic acids-based composites has been elaborated in Section 2.2. Generally, MOFs can act as an

efficient quencher to quench the fluorescence of the probe. In the presence of the target DNA or RNA molecules, the probe will be detached from the framework, hence recovering the fluorescence of the probe. For example, Zhang group developed several types of ultrathin 2D MOF nanosheets and applied for the fluorescence-based DNA detection [89]. The developed Cu-TCPP nanosheet with large surface area and thin thickness (4.5 ± 1.2 nm) could effectively absorb the dye-labeled single-stranded DNA (ssDNA, P1), leading to the fluorescence quenching by Förster resonance energy transfer (FRET) effect. In the presence of complementary DNA (T1), the double-stranded DNA (dsDNA) could be formed, resulting in the fluorescence recovery of dye molecules. Overall, this 2D platform presented excellent sensing performance with the detection limit of 20 pM and feasibility for simultaneous detection of multiple analytes (Fig. 12).

3.2. Catalysis

Due to the successful immobilization of enzyme on the MOFs, the enzyme-MOFs endow them with better performances in many aspects, especially in the heterogenous biocatalysis. As discussed in the Section 2.3.1, the developed MP-11@Tb-mesoMOF was applied to catalyze the oxidation of the substrate 3,5-dit-butyl-catechol (DTBC) in methanol/H_2O_2 solutions [68]. Due to its great solvent adaptability, the MP-11@Tb-mesoMOF presented a much higher conversion (48.7%) of o-quinone than that with free enzyme

(12.2%) (Fig. 13a). Later, Zhou group developed the enzyme-immobilized PCN-333 composite for the oxidation of o-phenylenediamine catalyzed by HRP or 2-2'-azino-bis(3-ethylbenz thiazoline-6-sulfonic acid) catalyzed by Cyt c and MP-11 [71].

The Farha group employed the water-stable mesoporous zirconium MOF, PCN-128y to encapsulate organophosphorus acid anhydrolase (OPAA), a nerve agent detoxifying enzyme which can hydrolyze the P-F, P-O, P-CN, and P-S bonds of toxic organophosphorus compounds [92]. The nerve agent simulant diisopropyl fluorophosphate (DFP) and the real toxic nerve agent O-pinacolyl methyl fluorophosphonate (Soman) were chosen as the model substrates. In the channel-type structure of MOFs, the large channels allow the efficient OPAA loading, while smaller ones facilitate the diffusion of reactants and products. Results indicated that OPAA@PCN-128y exhibited very high conversion efficiency (up to 90%) and remarkable thermal and long-term storage stability. Recently, Rafiei *et al.* developed a heterogeneous bio-catalyst by *in situ* encapsulation of Candida rugose lipase (CRL) into ZIF-67 [93]. Such biocompatible lipase@ZIF-67 enabled the promising transesterification of soybean oil to biodiesel. Hu *et al.* recently developed a polydimethylsiloxane (PDMS)-coated UiO-66 as the hydrophobic support for the immobilization of *Aspergillus niger* lipase (ANL) *via* hydrophobic interactions [94]. The hydrophobic modification strongly enhanced the enzymatic activity of ANL and the obtained ANL/UiO-66-PDMS-6 h exhibited high yield (88% at 24 h) in the lipase-catalyzed biodiesel production.
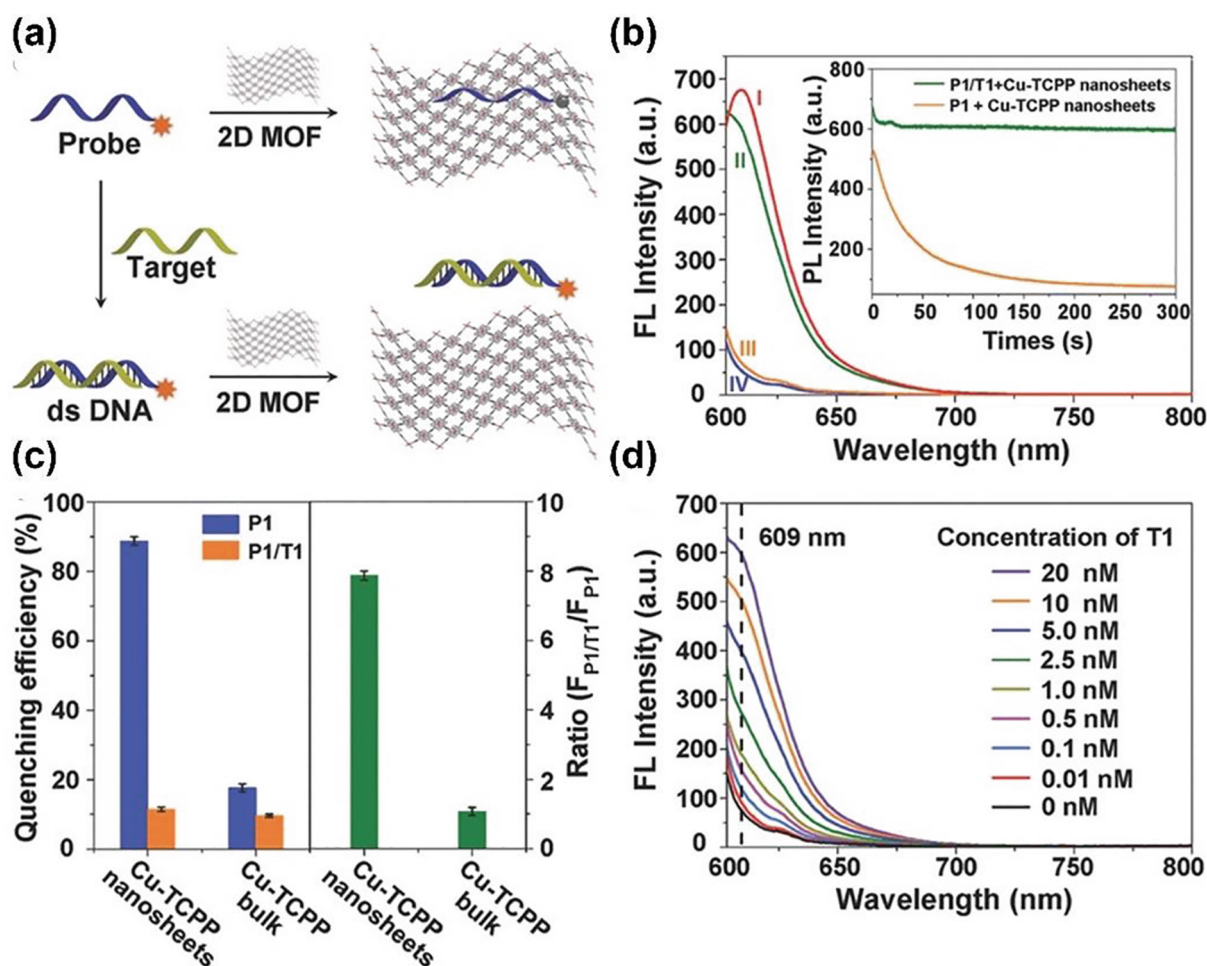

Fig.12. (a) Schematic illustration of DNA sensing using 2D MOF. (b)The fluorescence intensity of (I) P1(Texas red-labeled ssDNA), (II) P1 + Cu-TCPP + complementary DNA (T1), (III) P1 + Cu-TCPP, (IV) Cu-TCPP. (c) Quenching efficiency and fluorescence chemistry ratio in the presence of MOF nanosheets or bulk MOFs (d) Fluorescence recovery when treated with different concentrations of T1. Reprinted with permission from Ref. [89]. Copyright 2015, Viley-CH.
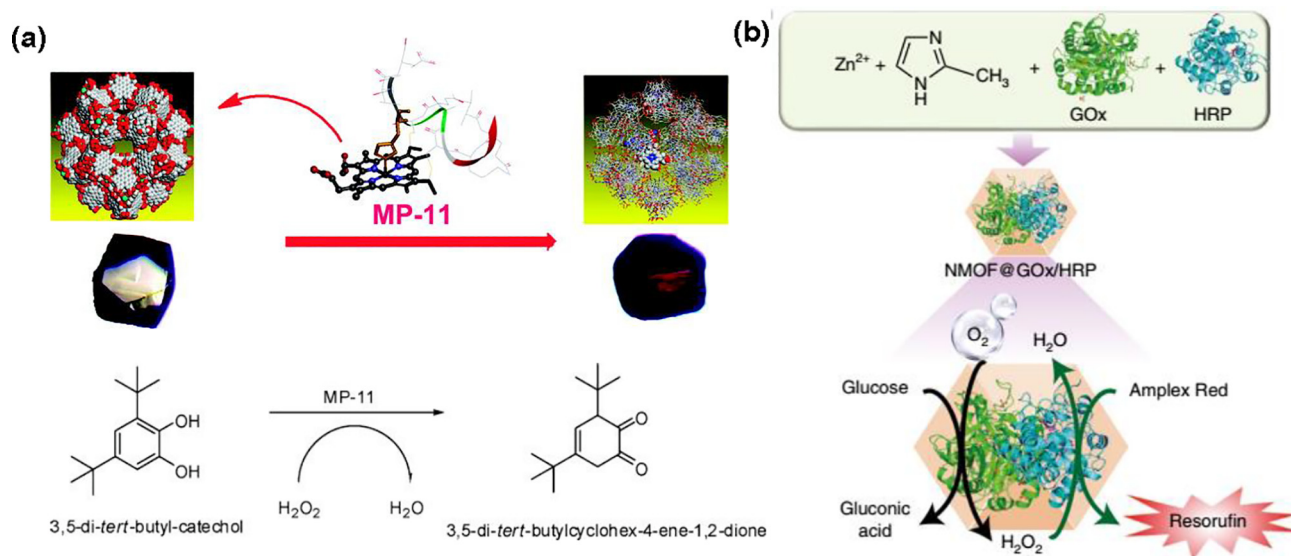
Fig. 13. (a) Schematic illustration of MP-11 immobilization on MOF to obtain MP-11@mesoMOF and MP-11 mediated catalytical reactions. Reprinted with permission from Ref. [68]. Copyright 2011, American Chemical Society. (b) Catalytic cascade reactions driven by NMOF@GOx/HRP nanoreactor. Reprinted with permission from Ref. [95]. Copyright 2018, Nature Publishing Group.

Willner group did an excellent work on the encapsulation of two or three enzymes into ZIF8-NMOFs for biologically catalytic cascades [95]. As one of the model reactions in Fig. 13b, two enzymes, GOx and HRP were loaded into the NMOFs at the same time. In the presence of GOx, glucose could be oxidized to gluconic acid and H_2O_2. The generated H_2O_2 immediately initiated the oxidation of Amplex Red to the fluorescent resorufin under the catalysis of HRP. Beyond that, integration of three enzymes (β-galactosidase, GOx and HRP) or enzyme/cofactor components (alcohol dehydrogenase, NAD^+-functionalized polymer and NAD^+-dependent lactate dehydrogenase) was also successfully acheived. The subsequent catalytic activities implied that this NMOF nanoreactor could facilitate the effective intercommunication between enzymes.

3.3. Molecular imaging

Due to the strong tailorable chemistry of NCPs, metal ions or organic linkers with the imaging characteristics could be incorporated into structure for the molecular imaging purpose [96–99]. For example, the Fe^{3+}, Gd^{3+} and Mn^{2+} containing NCPs have been widely explored for magnetic resonance imaging (MRI) [100–103]. Also, the high Z number elements such as iodine (I), hafnium (Hf) and bismuth (Bi) have been applied to construct NCPs for X-ray computed tomography (CT) imaging [104–106]. Lanthanide cations with narrow emission bands allow to create the fluorescent NCPs for cell or tissue imaging [107]. In terms of organic building units, bioimaging can also be achieved by utilizing the intrinsically fluorescent NCPs (like porphyrin-based MOFs) or loading organic fluorophores into the structure. Moreover, some NCPs can be tuned by combining multiple metal ions or dyes for the multimodality imaging [108–112].

Recently, Yan group assembled the biliverdin (BV), the endogenous metabolic product of heme, Z-Histidine-Obzl (ZHO) and Mn^{2+} into a NCP-based NIR photothermal nanoagent [113]. BV was chosen due to its broad NIR absorption, clear metabolic pathways and high photothermal conversion efficiency, which can be applied for the photoacoustic imaging (PAI) and photothermal therapy. The imidazole side chain in ZHO could coordinate with metal ions and thus tune the assembly process. Additionally, MRI imaging could be achieved by incorporation of Mn^{2+}. The formed NCPs

demonstrated well-defined morphology, colloidal stability and prolonged blood circulation. Importantly, this multifunctional nanomaterial was able to selectively accumulate in tumors, leading to efficient PAI/MR imaging and further photothermal ablation of cancer cells. By taking advantages of superior benefits of individual imaging techniques, multimodality imaging could provide more comprehensive and complementary information, which could further facilitate the imaging-guided therapy (Fig. 14).

NCPs with π-electron system can work as the efficient quenchers to quench the fluorescence of dye-based probes. Wu et al. presented a nanoscale MOFs for the multiplexed miRNAs sensing in living cells. The system consisted of dye-labeled peptide nucleic acid (PNA) probe and MOF as the quencher. In the presence of target miRNA, the hybridized PNA is detached from MOF, leading to the recovery of fluorescence [57]. Recently, Liu et al. used a phosphate-terminal DNA aptamer labeled with TAMRA to conjugate with ZrMOF nanoparticle quencher for target-induced bioimaging [114]. Phosphate group coupled to the 5′ end of the aptamer could effectively coordinate with zirconium, leading to the proximity of TAMRA and MOF. Hence fluorescence would be recovered when treated with the complementary DNA (cDNA), resulting in the target-induced imaging in live cells and photodynamic therapy thereafter.

When NCPs are fabricated with other nanomaterials, the formed composite could combine both advantages of NCPs and nanomaterials, hence expanding their use in the biological applications [108,110]. Ju group developed a core-shell nanostructure via integrating pH-responsive MOFs with enzyme-responsive peptide-modified gold nanoparticles (AuNPs) [115]. The ZIF-8 shell could be decomposed under acidic conditions, resulting in the exposure of peptide-conjugated AuNPs. On the other hand, Cyanine 3 (Cy3)-labeled peptide (Cy3-GRRGKC) could be recognized by the Cathepsin B (CaB) enzyme, leading to the liberated fluorescence of Cy3 from AuNPs. This Au-Cy3P@ZIF-8 composite eventually achieved sequential response and localized fluorescence imaging in the acidic lysosome, where the CaB is mainly located.

3.4. Delivery and therapy

Due to the large surface area and highly porous structure, NCPs can serve as the optimal carriers for loading of versatile cargos,
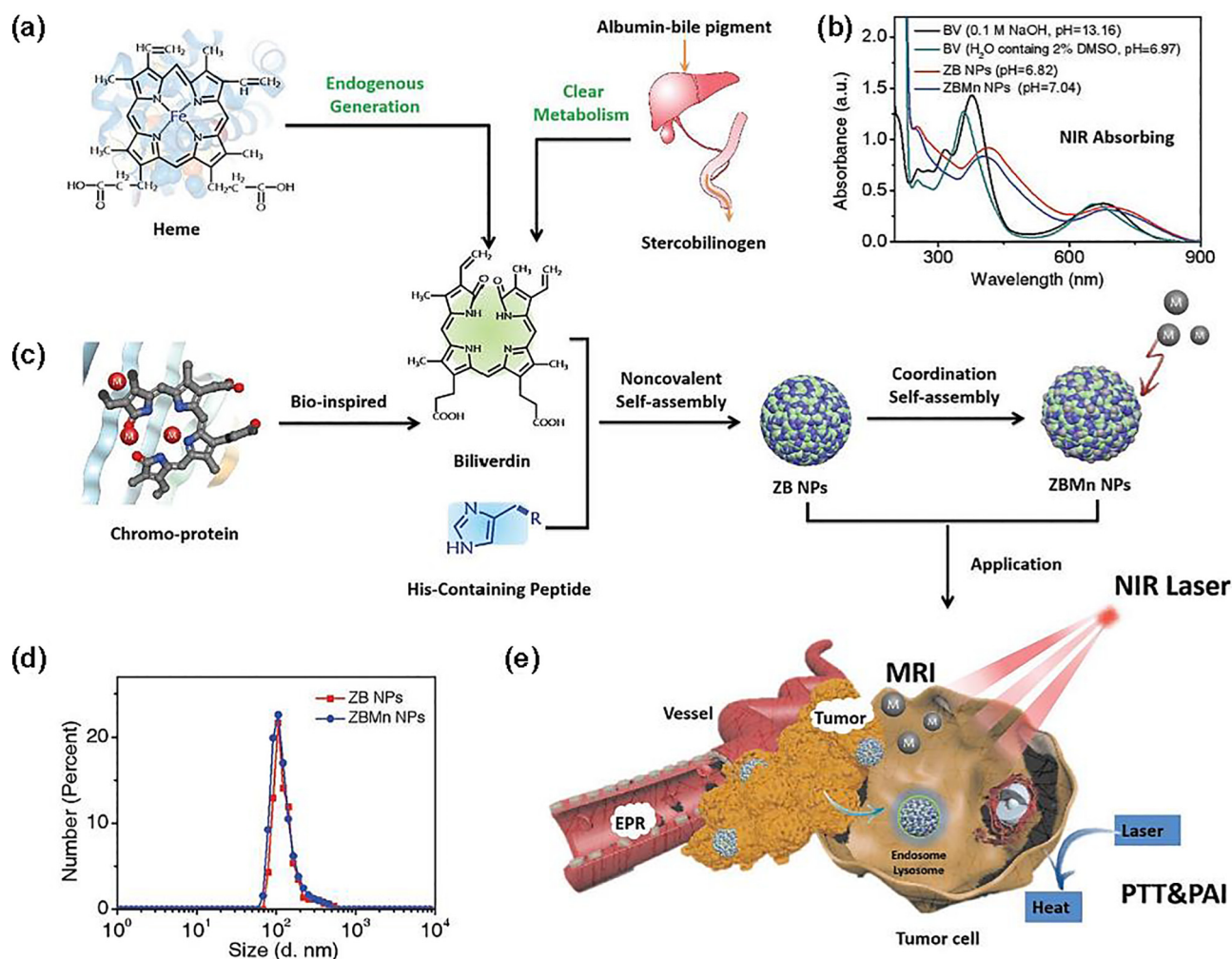
Fig. 14. (a) Schematic illustration of biliverdin (BV)-derived ZBMn NPs for multimodal tumor imaging and therapy. Reprinted with permission from Ref. [113]. Copyright 2019, Viley-CH.

including imaging regents, enzymes, drugs, genes and other therapeutic agents. Currently, NCPs or MOFs have been extensively applied in drug delivery and cancer and other disease-related therapy [8,116–118].

Lin group developed UiO NMOFs with aminotriphenyldicarboxylic acid (amino-TPDC) bridging ligand for the co-delivery of cisplatin prodrug and pooled siRNAs [59]. The prodrug could be first encapsulated into the large pores of NMOFs, followed by the siRNA loading on the surface site due to coordination binding with metal ions. Results demonstrated that nanoscale UiO-66 MOFs could effectively prevent the siRNA from degradation and greatly enhance the cellular uptake and lysosome escape. The in vitro cell assays demonstrated that the co-delivery could greatly improve the therapeutic efficacy in cisplatin-resistant ovarian cancer cells (Fig. 15a). For the delivery of nucleic acids, Fan group prepared the immunostimulatory oligonucleotides cytosine-phosphate-guanosine (CpG)-MOFs, which was further modified with calcium phosphate (CaP) exoskeleton (Fig. 15b) [119]. The UiO-66 MOF structure exhibited the optimal carrier behaviors with high loading capacity and efficient intracellular delivery. CaP exoskeleton played the protective roles in physiological conditions, while were degraded in acidic endolysosomes. Moreover, the generated phosphate ions would further trigger the on-demand release of DNA. More recently, Tang group explored the intracellular delivery of plasmid DNA (pDNA) with ZIF-8 [120]. The in vitro experiment

indicated improved gene transportation and expression by using the MOF-based non-viral vectors.

Zhang group developed a one-pot, and organic solvent-free post-synthetic method for MOF-based drug delivery systems (DDS) [121]. Firstly, doxorubicin (Dox) was loaded in the azide-modified MOF MIL-101-N₃(Fe). Subsequently, bicyclononyne (BCN) functionalized β-cyclodextrin (β-CD) derivative (β-CD-SS-BCN) was conjugated with MOF via the copper free click chemistry. Additionally, peptide functionalized polymer Lys(adamantane)-Arg-Gly-Asp-Ser-bi-PEG1900 (bi = benzoic imine bond, K(ad)RGDS-PEG1900) can be linked to the surface through the host–guest interactions between β-CD and adamantane. The benzoic imine bond could be cleaved under acidic conditions, resulting in the exposure of shielded RGD peptide for $\alpha v\beta_3$ integrin targeting. Later, β-CD could be removed under reducing conditions (e.g. Glutathione (GSH)) due to the presence of disulfide bond. Results implied that such dual-responsive DDS exhibited enhanced tumor uptake and controlled drug release.

As mentioned above, the enzyme-MOF composites have been applied for the sensing and catalysis, one interesting example is that they can also be used as the nanoreactor for prodrug activation. Zhou group developed tyrosinase encapsulated PCN-333(Al) (TYR@NPCN-333) to activate the cancer prodrug paracetamol (APAP) [123]. Results suggested that both nanoreactor and prodrug would not cause obvious toxic effect, while enzyme-catalyzed
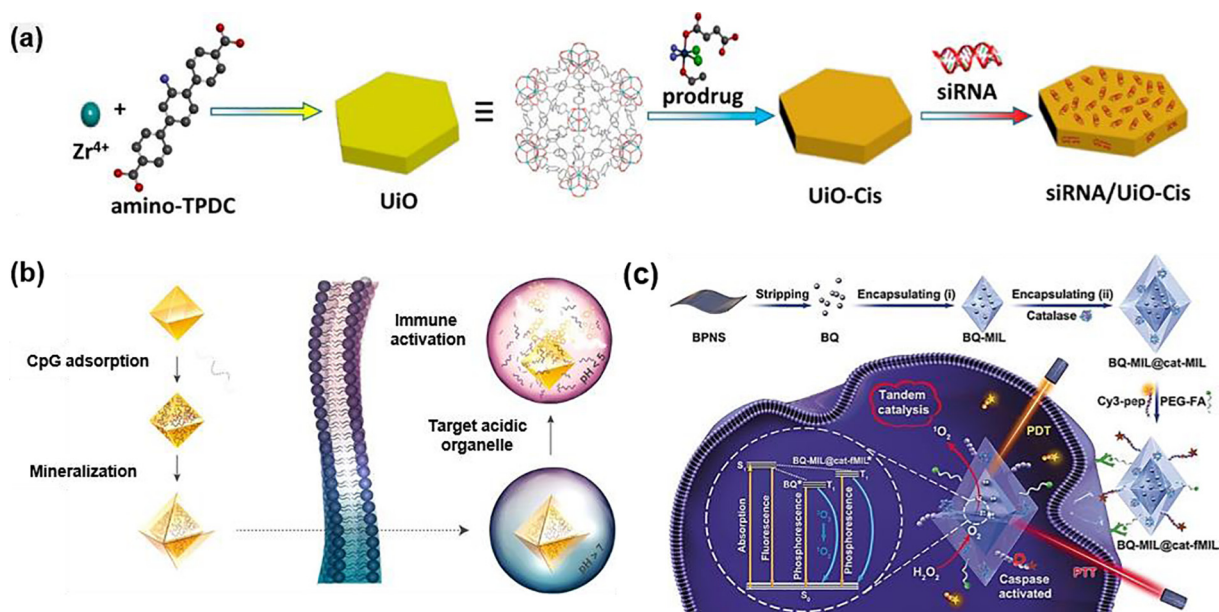
Fig. 15. (a) Schematic illustration on the presentation of siRNA/UiO-Cis. Reprinted with permission from Ref. [59]. Copyright 2014, American Chemical Society. (b) Schematic preparation of immunostimulatory DNA − MOFs (isMOFs) and stimulated immune responses [119] Copyright 2017, American Chemical Society. (c) The preparation of BQ and catalase immobilized MOF for improved therapy [122]. Copyright 2019, Viley-CH.

product 4-acetamido-o-benzoquinone (AOBQ) will severely induce the generation of reactive oxygen species (ROS) and GSH depletion. Therefore, MOF encapsulation could help prolong the activity time in cells and tumors, hence promoting the antitumor efficacy of APAP. More recently, Liu *et al.* used Lavoisier (MIL-101)-type MOF to simultaneously delivery black phosphorus quantum dot (BQ) and catalase to achieve the photodynamic-thermal synergistic effect (Fig. 15c) [122]. Initially, the catalase immobilized on the outer layer could catalyze the intracellular H_2O_2 to O_2, which could subsequently assist the BQ-based PDT with extra oxygen supply. The BQ-mediated photodynamic-thermal synergistic therapy resulted in obvious apoptotic process and activation of caspase-3, leading to the turn-on fluorescence signals for monitoring of the therapeutic efficacy.

4. Conclusions and perspectives

The past decades have seen the explosive growth in NCPs for various applications. In particular, the engineering of NCPs with biomolecules has attracted great attention in material science, chemistry and biological fields. Currently, a variety of biomolecules including amino acids, peptides, nucleic acids, enzymes and lipids have been incorporated into NCPs or NMOFs. Basically, the immobilization approaches include complexation as building units, physical encapsulation or absorption, covalent conjugation and *de novo* method. Among these approaches, the covalent conjugation usually requires some functional groups like amine or carboxylate groups in NCPs, which can link with biomolecules *via* coupling reactions. In terms of the other methods, the coordination chemistry *via* π-π stacking, electrostatic interactions, and H-bonding *etc.* is the main force to create strong interactions between biomolecules and NCPs. Compared to free biomolecules, the formed bio-composites are advantageous in several aspects: i) extra protection from NCPs could greatly enhance the thermal and storage stability of biomolecules; ii) the tolerance to organic solvent or other harsh conditions could be significantly enhanced; iii) increased catalytic activities and reusability could be achieved

for many types of enzymes. More importantly, the integration of NCP and biomolecules endow the bio-composites with combined functionalities and more advanced applications. Till now, several promising applications of biomolecule-NCP composites have been explored, including biosensing, catalysis, molecular imaging and drug delivery *etc.*

Despite the remarkable achievements that have been made in the biomolecule-integrated NCP hybrid materials, several unsolved issues still exist. Current established approaches, though, have offered multiple choices for the immobilization of biomolecules, each of them has its pros and cons. Biomolecules used as building ligands to construct the bio-composites are quite limited, and only a few types of small biomolecules like amino acids, short peptides and nucleobases can be applied *via* this method. Also, the strong coordination bonds between metals and biomolecules may potentially cause the structural or conformational changes and restrict their subsequent activities. Covalent conjugation seems a good strategy to maintain the molecular conformation and avoid the unwanted leakage of biomolecules, while functional groups in the NCPs are required for later chemical reaction. Additionally, further modification on biomolecules is necessary if the amino or carboxylate groups are not contained in the structure. Moreover, the coupling efficiency is limited in many cases and new synthetic methods may need to be further explored. The physical encapsulation approach has no special requirement on any functional groups in host NCPs. However, the rigid porous structure may either cause the leakage of some biomolecules, whose size is much smaller than pore size, or prevent the large biomolecules from loading into the cavity. The other method, *de novo* approach may compensate the shortage on the size limitation for guest molecules, which can be simultaneously embedded inside the NMOFs through one pot synthesis. However, the low tolerance of biomolecules to high temperature or organic solvents restrict the synthesis to be conducted under mild conditions, in which most NCPs are difficult to be obtained. Therefore, optimization of current synthetic strategies or exploration of new approaches to broadening the spectrum of bio-composites are critical to push forward the development of biomolecule-based NCP materials.

Apart from the engineering of biomolecules into NCPs, other essential factors should also be considered. The pore size of currently developed NCPs is relatively small, which only can encapsulate certain types of biomolecules. Hence, further explorations of mesoporous NCPs with larger pore sizes are required. Also, the control of the pore size is of significance for effective interactions between biomolecules with surrounding species in the applications of sensing and catalysis. Additionally, it is still questionable to maintain the activities of biomolecule after the successful loading into NCPs. The unfriendly reaction conditions may cause the conformational changes or degradation of biomolecules. Therefore, either preventing biomolecules from the exposure to harsh conditions or stabilizing the NCPs in biomolecule-favored conditions are possible ways to solve this problem. In order to make the NCPs act as ideal platforms for more advanced bio-applications, the *in situ* release of biomolecules into biological sites from the NCPs should be investigated. The balance between effective trapping into the NCPs and controlled release to fulfill biological functions of biomolecules should be managed properly. Last but not the least, the biocompatibility of formed hybrid materials should be carefully evaluated before its future biomedical use.

In summary, biomolecule-NCP composites with intriguing features have made great achievements in many fields. The structure and functionality diversity of NCP-based hybrid materials provide great potentials in future applications in both industry and biomedicine.

Declaration of Competing Interest

The authors declare that they have no known competing financial interests or personal relationships that could have appeared to influence the work reported in this paper.

Acknowledgements

Appendix A. Supplementary data

Supplementary data to this article can be found online at https://doi.org/10.1016/j.ccr.2019.213039.

References

[1] C. He, D. Liu, W. Lin, Chem. Rev. 115 (2015) 11079–11108.
[2] M. Giménez-Marqués, T. Hidalgo, C. Serre, P. Horcajada, Coord. Chem. Rev. 307 (2016) 342–360.
[3] B. Li, S.-Q. Zang, L.-Y. Wang, T.C.W. Mak, Coord. Chem. Rev. 308 (2016) 1–21.
[4] H. Li, K. Wang, Y. Sun, C.T. Lollar, J. Li, H.-C. Zhou, Mater. Today 21 (2018) 108–121.
[5] H. Wang, Q.-L. Zhu, R. Zou, Q. Xu, Chem 2 (2017) 52–80.
[6] Y.-Z. Chen, R. Zhang, L. Jiao, H.-L. Jiang, Coord. Chem. Rev. 362 (2018) 1–23.
[7] Q. Qiu, H. Chen, Y. Wang, Y. Ying, Coord. Chem. Rev. 387 (2019) 60–78.
[8] M.X. Wu, Y.W. Yang, Adv. Mater. 29 (2017) 1606134.
[9] K. Lu, T. Aung, N. Guo, R. Weichselbaum, W. Lin, Adv. Mater. 30 (2018) 1707634.
[10] M.I. Nandasiri, S.R. Jambovane, B.P. McGrail, H.T. Schaef, S.K. Nune, Coord. Chem. Rev. 311 (2016) 38–52.
[11] S. Begum, Z. Hassan, S. Bräse, C. Wöll, M. Tsotsalas, Acc. Chem. Res. 52 (2019) 1598–1610.
[12] Y. Liu, Y. Zhao, X. Chen, Theranostics 9 (2019) 3122.
[13] W. Xiang, Y. Zhang, H. Lin, C.-J. Liu, Molecules (Basel, Switzerland) 22 (2017) 2103.
[14] P. Shivcharan, R. Ipsita, Recent Pat. Biotechnol. 12 (2018) 33–56.
[15] S. Ulrich, P. Dumy, D. Boturyn, O. Renaudet, J. Drug Deliv. Sci. Technol. 23 (2013) 5–16.
[16] M.I. Gibson, M.R. Seyedsayamdost, ACS Cent. Sci. 4 (2018) 437–439.
[17] A. Schmid, J.S. Dordick, B. Hauer, A. Kiener, M. Wubbolts, B. Witholt, Nature 409 (2001) 258–268.
[18] D.C. Chow, M.S. Johannes, W.-K. Lee, R.L. Clark, S. Zauscher, A. Chilkoti, Mater. Today 8 (2005) 30–39.
[19] T. Nagamune, Nano Converg. 4 (2017) 9.
[20] K. Liang, J.J. Richardson, J. Cui, F. Caruso, C.J. Doonan, P. Falcaro, Adv. Mater. 28 (2016) 7910–7914.
[21] H. Cai, Y.-L. Huang, D. Li, Coord. Chem. Rev. 378 (2019) 207–221.
[22] J. Zhuang, A.P. Young, C.K. Tsung, Small 13 (2017) 1700880.
[23] H. An, M. Li, J. Gao, Z. Zhang, S. Ma, Y. Chen, Coord. Chem. Rev. 384 (2019) 90–106.
[24] S.L. Anderson, K.C. Stylianou, Coord. Chem. Rev. 349 (2017) 102–128.
[25] B. Li, H.-M. Wen, Y. Cui, W. Zhou, G. Qian, B. Chen, Adv. Mater. 28 (2016) 8819–8860.
[26] Y. Cui, B. Li, H. He, W. Zhou, B. Chen, G. Qian, Acc. Chem. Res. 49 (2016) 483–493.
[27] Q.-L. Zhu, Q. Xu, Chem. Soc. Rev. 43 (2014) 5468–5512.
[28] Z. Zhou, M. Hartmann, Chem. Soc. Rev. 42 (2013) 3894–3912.
[29] J. Li, X. Wang, G. Zhao, C. Chen, Z. Chai, A. Alsaedi, T. Hayat, X. Wang, Chem. Soc. Rev. 47 (2018) 2322–2356.
[30] I. Imaz, M. Rubio-Martinez, J. An, I. Sole-Font, N.L. Rosi, D. Maspoch, Chem. Commun. 47 (2011) 7287–7302.
[31] L. Chen, X. Bu, Chem. Mater. 18 (2006) 1857–1860.
[32] J. Rabone, Y.-F. Yue, S. Chong, K. Stylianou, J. Bacsa, D. Bradshaw, G. Darling, N. Berry, Y. Khimyak, A. Ganin, Science 329 (2010) 1053–1057.
[33] C. Martí-Gastaldo, J.E. Warren, K.C. Stylianou, N.L. Flack, M.J. Rosseinsky, Angew. Chem. Int. Ed. 51 (2012) 11044–11048.
[34] A.P. Katsoulidis, K.S. Park, D. Antypov, C. Martí-Gastaldo, G.J. Miller, J.E. Warren, C.M. Robertson, F. Blanc, G.R. Darling, N.G. Berry, Angew. Chem. Int. Ed. 53 (2014) 193–198.
[35] J. Navarro-Sánchez, A.I. Argente-García, Y. Moliner-Martínez, D. Roca-Sanjuán, D. Antypov, P. Campins-Falco, M.J. Rosseinsky, C. Marti-Gastaldo, J. Am. Chem. Soc. 139 (2017) 4294–4297.
[36] Y. Ikezoe, G. Washino, T. Uemura, S. Kitagawa, H. Matsui, Nat. Mater. 11 (2012) 1081.
[37] Y. Ikezoe, J. Fang, T.L. Wasik, M. Shi, T. Uemura, S. Kitagawa, H. Matsui, Nano Lett. 15 (2015) 4019–4023.
[38] W. Ma, L. Xu, Z. Li, Y. Sun, Y. Bai, H. Liu, Nanoscale 8 (2016) 10908–10912.
[39] H. Hintz, S. Wuttke, Chem. Commun. 50 (2014) 11472–11475.
[40] J. Bonnefoy, A. Legrand, E.A. Quadrelli, J.r.m. Canivet, D. Farrusseng, J. Am. Chem. Soc. 137 (2015) 9409–9416.
[41] A.M. Fracaroli, P. Siman, D.A. Nagib, M. Suzuki, H. Furukawa, F.D. Toste, O.M. Yaghi, J. Am. Chem. Soc. 138 (2016) 8352–8355.
[42] P. Amo-Ochoa, F. Zamora, Coord. Chem. Rev. 276 (2014) 34–58.
[43] M. Zhang, Z.-Y. Gu, M. Bosch, Z. Perry, H.-C. Zhou, Coord. Chem. Rev. 293–294 (2015) 327–356.
[44] J. An, S.J. Geib, N.L. Rosi, J. Am. Chem. Soc. 131 (2009) 8376–8377.
[45] J. An, O.K. Farha, J.T. Hupp, E. Pohl, J.I. Yeh, N.L. Rosi, Nat. Commun. 3 (2012) 604.
[46] M. Zhang, W. Lu, J.-R. Li, M. Bosch, Y.-P. Chen, T.-F. Liu, Y. Liu, H.-C. Zhou, Inorgan. Chem. Front. 1 (2014) 159–162.
[47] M. Li, C. Wang, Z. Di, H. Li, J. Zhang, W. Xue, M. Zhao, K. Zhang, Y. Zhao, L. Li, Angew. Chem. Int. Ed. 58 (2019) 1350–1354.
[48] W. Morris, W.E. Briley, E. Auyeung, M.D. Cabezas, C.A. Mirkin, J. Am. Chem. Soc. 136 (2014) 7261–7264.
[49] J.S. Kahn, L. Freage, N. Enkin, M.A.A. Garcia, I. Willner, Adv. Mater. 29 (2017) 1602782.
[50] L. He, M. Brasino, C. Mao, S. Cho, W. Park, A.P. Goodwin, J.N. Cha, Small 13 (2017) 1700504.
[51] S. Wang, C.M. McGuirk, M.B. Ross, S. Wang, P. Chen, H. Xing, Y. Liu, C.A. Mirkin, J. Am. Chem. Soc. 139 (2017) 9827–9830.
[52] S. Wang, Y. Chen, S. Wang, P. Li, C.A. Mirkin, O.K. Farha, J. Am. Chem. Soc. 141 (2019) 2215–2219.
[53] L. Chen, H. Zheng, X. Zhu, Z. Lin, L. Guo, B. Qiu, G. Chen, Z.-N. Chen, Analyst 138 (2013) 3490–3493.
[54] X. Wei, L. Zheng, F. Luo, Z. Lin, L. Guo, B. Qiu, G. Chen, J. Mater. Chem. B 1 (2013) 1812–1817.
[55] X. Zhu, H. Zheng, X. Wei, Z. Lin, L. Guo, B. Qiu, G. Chen, Chem. Commun. 49 (2013) 1276–1278.
[56] T. Ye, Y. Liu, M. Luo, X. Xiang, X. Ji, G. Zhou, Z. He, Analyst 139 (2014) 1721–1725.
[57] Y. Wu, J. Han, P. Xue, R. Xu, Y. Kang, Nanoscale 7 (2015) 1753–1759.
[58] Y. Jia, B. Wei, R. Duan, Y. Zhang, B. Wang, A. Hakeem, N. Liu, X. Ou, S. Xu, Z. Chen, X. Lou, F. Xia, Sci. Rep. 4 (2014) 5929.
[59] C. He, K. Lu, D. Liu, W. Lin, J. Am. Chem. Soc. 136 (2014) 5181–5184.
[60] S. Peng, B. Bie, Y. Sun, M. Liu, H. Cong, W. Zhou, Y. Xia, H. Tang, H. Deng, X. Zhou, Nat. Commun. 9 (2018) 1293.
[61] I. Schomburg, A. Chang, S. Placzek, C. Söhngen, M. Rother, M. Lang, C. Munaretto, S. Ulas, M. Stelzer, A. Grote, M. Scheer, D. Schomburg, Nucleic Acids Res. 41 (2013) D764–D772.
[62] M. Vellard, Curr. Opin. Biotechnol. 14 (2003) 444–450.

[63] O. Kirk, T.V. Borchert, C.C. Fuglsang, Curr. Opin. Biotechnol. 13 (2002) 345–351.
[64] A.A. Homaei, R. Sariri, F. Vianello, R. Stevanato, J. Chem. Biol. 6 (2013) 185–205.
[65] X. Lian, Y. Fang, E. Joseph, Q. Wang, J. Li, S. Banerjee, C. Lollar, X. Wang, H.-C. Zhou, Chem. Soc. Rev. 46 (2017) 3386–3401.
[66] T.J. Pisklak, M. Macías, D.H. Coutinho, R.S. Huang, K.J. Balkus, Top. Catal. 38 (2006) 269–278.
[67] W. Ma, Q. Jiang, P. Yu, L. Yang, L. Mao, Anal. Chem. 85 (2013) 7550–7557.
[68] V. Lykourinou, Y. Chen, X.-S. Wang, L. Meng, T. Hoang, L.-J. Ming, R.L. Musselman, S. Ma, J. Am. Chem. Soc. 133 (2011) 10382–10385.
[69] Y. Chen, V. Lykourinou, T. Hoang, L.-J. Ming, S. Ma, Inorg. Chem. 51 (2012) 9156–9158.
[70] Y. Chen, V. Lykourinou, C. Vetromile, T. Hoang, L.-J. Ming, R.W. Larsen, S. Ma, J. Am. Chem. Soc. 134 (2012) 13188–13191.
[71] D. Feng, T.-F. Liu, J. Su, M. Bosch, Z. Wei, W. Wan, D. Yuan, Y.-P. Chen, X. Wang, K. Wang, X. Lian, Z.-Y. Gu, J. Park, X. Zou, H.-C. Zhou, Nat. Commun. 6 (2015) 5979.
[72] S. Jung, Y. Kim, S.-J. Kim, T.-H. Kwon, S. Huh, S. Park, Chem. Commun. 47 (2011) 2904–2906.
[73] Y.-H. Shih, S.-H. Lo, N.-S. Yang, B. Singco, Y.-J. Cheng, C.-Y. Wu, I.-H. Chang, H.-Y. Huang, C.-H. Lin, ChemPlusChem 77 (2012) 982–986.
[74] C. Tudisco, G. Zolubas, B. Seoane, H.R. Zafarani, M. Kazemzad, J. Gascon, P.L. Hagedoorn, L. Rassaei, RSC Adv. 6 (2016) 108051–108055.
[75] F. Lyu, Y. Zhang, R.N. Zare, J. Ge, Z. Liu, Nano Lett. 14 (2014) 5761–5765.
[76] F.-K. Shieh, S.-C. Wang, C.-I. Yen, C.-C. Wu, S. Dutta, L.-Y. Chou, J.V. Morabito, P. Hu, M.-H. Hsu, K.C.-W. Wu, J. Am. Chem. Soc. 137 (2015) 4276–4279.
[77] K. Liang, R. Ricco, C.M. Doherty, M.J. Styles, S. Bell, N. Kirby, S. Mudie, D. Haylock, A.J. Hill, C.J. Doonan, P. Falcaro, Nat. Commun. 6 (2015) 7240.
[78] S.K. Alsaiari, S. Patil, M. Alyami, K.O. Alamoudi, F.A. Aleisa, J.S. Merzaban, M. Li, N.M. Khashab, J. Am. Chem. Soc. 140 (2017) 143–146.
[79] T.-T. Chen, J.-T. Yi, Y.-Y. Zhao, X. Chu, J. Am. Chem. Soc. 140 (2018) 9912–9920.
[80] Z. Wang, S. Hu, J. Yang, A. Liang, Y. Li, Q. Zhuang, J. Gu, Adv. Funct. Mater. 28 (2018) 1707356.
[81] P. Li, Justin A. Modica, Ashlee J. Howarth, E. Vargas L, Peyman Z. Moghadam, Randall Q. Snurr, M. Mrksich, Joseph T. Hupp, Omar K. Farha, Chem 1 (2016) 154–169.
[82] W. Liang, H. Xu, F. Carraro, N.K. Maddigan, Q. Li, S.G. Bell, D.M. Huang, A. Tarzia, M.B. Solomon, H. Amenitsch, L. Vaccari, C.J. Sumby, P. Falcaro, C.J. Doonan, J. Am. Chem. Soc. 141 (2019) 2348–2355.
[83] R.C. Huxford-Phillips, S.R. Russell, D. Liu, W. Lin, RSC Adv. 3 (2013) 14438–14443.
[84] D. Liu, C. Poon, K. Lu, C. He, W. Lin, Nat. Commun. 5 (2014) 4182.
[85] C. He, D. Liu, W. Lin, ACS Nano 9 (2015) 991–1003.
[86] S. Wuttke, S. Braig, T. Preiß, A. Zimpel, J. Sicklinger, C. Bellomo, J.O. Rädler, A. M. Vollmar, T. Bein, Chem. Commun. 51 (2015) 15752–15755.
[87] C. Hou, Y. Wang, Q. Ding, L. Jiang, M. Li, W. Zhu, D. Pan, H. Zhu, M. Liu, Nanoscale 7 (2015) 18770–18779.
[88] Y. Yin, C. Gao, Q. Xiao, G. Lin, Z. Lin, Z. Cai, H. Yang, ACS Appl. Mater. Interfaces 8 (2016) 29052–29061.
[89] M. Zhao, Y. Wang, Q. Ma, Y. Huang, X. Zhang, J. Ping, Z. Zhang, Q. Lu, Y. Yu, H. Xu, Y. Zhao, H. Zhang, Adv. Mater. 27 (2015) 7372–7378.
[90] S. Wu, H. Min, W. Shi, P. Cheng, Adv. Mater. (2019) 1805871.
[91] W. Chen, W. Yang, Y. Lu, W. Zhu, X. Chen, Anal. Methods 9 (2017) 3213–3220.
[92] P. Li, S.-Y. Moon, M.A. Guelta, S.P. Harvey, J.T. Hupp, O.K. Farha, J. Am. Chem. Soc. 138 (2016) 8052–8055.
[93] S. Rafiei, S. Tangestaninejad, P. Horcajada, M. Moghadam, V. Mirkhani, I. Mohammadpoor-Baltork, R. Kardanpour, F. Zadehahmadi, Chem. Eng. J. 334 (2018) 1233–1241.
[94] Y. Hu, L. Dai, D. Liu, W. Du, Green Chem. 20 (2018) 4500–4506.
[95] W.-H. Chen, M. Vazquez-Gonzalez, A. Zoabi, R. Abu-Reziq, I. Willner, Nat. Catal. 1 (2018) 689.
[96] J. Della Rocca, D. Liu, W. Lin, Acc. Chem. Res. 44 (2011) 957–968.
[97] P. Horcajada, T. Chalati, C. Serre, B. Gillet, C. Sebrie, T. Baati, J.F. Eubank, D. Heurtaux, P. Clayette, C. Kreuz, Nat. Mater. 9 (2010) 172–180.
[98] D. Liu, R.C. Huxford, W. Lin, Angew. Chem. Int. Ed. 50 (2011) 3696–3700.
[99] H.-S. Wang, Coord. Chem. Rev. 349 (2017) 139–155.
[100] H.-X. Zhao, Q. Zou, S.-K. Sun, C. Yu, X. Zhang, R.-J. Li, Y.-Y. Fu, Chem. Sci. 7 (2016) 5294–5301.
[101] K.M.L. Taylor, A. Jin, W. Lin, Angew. Chem. Int. Ed. 47 (2008) 7722–7725.
[102] K.M. Taylor, W.J. Rieter, W. Lin, J. Am. Chem. Soc. 130 (2008) 14358–14359.
[103] D. Wang, J. Zhou, R. Shi, H. Wu, R. Chen, B. Duan, G. Xia, P. Xu, H. Wang, S. Zhou, Theranostics 7 (2017) 4605.
[104] K.E. deKrafft, Z. Xie, G. Cao, S. Tran, L. Ma, O.Z. Zhou, W. Lin, Angew. Chem. Int. Ed. 48 (2009) 9901–9904.
[105] K.E. deKrafft, W.S. Boyle, L.M. Burk, O.Z. Zhou, W. Lin, J. Mater. Chem. 22 (2012) 18139–18144.
[106] L. Robison, L. Zhang, R.J. Drout, P. Li, C.R. Haney, A. Brikha, H. Noh, B.L. Mehdi, N.D. Browning, V.P. Dravid, Q. Cui, T. Islamoglu, O.K. Farha, ACS Appl. Biol. Mater. 2 (2019) 1197–1203.
[107] A. Foucault-Collet, K.A. Gogick, K.A. White, S. Villette, A. Pallier, G. Collet, C. Kieda, T. Li, S.J. Geib, N.L. Rosi, S. Petoud, Proc. Natl. Acad. Sci. U.S.A. 110 (2013) 17199.
[108] Y. Li, J. Tang, L. He, Y. Liu, Y. Liu, C. Chen, Z. Tang, Adv. Mater. 27 (2015) 4075–4080.
[109] Y.-M. Wang, W. Liu, X.-B. Yin, Adv. Funct. Mater. 26 (2016) 8463–8470.
[110] W. Shang, C. Zeng, Y. Du, H. Hui, X. Liang, C. Chi, K. Wang, Z. Wang, J. Tian, Adv. Mater. 29 (2017) 1604381.
[111] Y. Yang, Y. Chao, J. Liu, Z. Dong, W. He, R. Zhang, K. Yang, M. Chen, Z. Liu, NPG Asia Mater. 9 (2017) e344.
[112] Y.-M. Wang, W. Liu, X.-B. Yin, Chem. Sci. 8 (2017) 3891–3897.
[113] R. Xing, Q. Zou, C. Yuan, L. Zhao, R. Chang, X. Yan, Adv. Mater. 31 (2019) 1900822.
[114] Y. Liu, W. Hou, L. Xia, C. Cui, S. Wan, Y. Jiang, Y. Yang, Q. Wu, L. Qiu, W. Tan, Chem. Sci. 9 (2018) 7505–7509.
[115] H. Shen, J. Liu, J. Lei, H. Ju, Chem. Commun. 54 (2018) 9155–9158.
[116] C. Chu, M. Su, J. Zhu, D. Li, H. Cheng, X. Chen, G. Liu, Theranostics 9 (2019) 3134.
[117] A. Pöthig, A. Casini, Theranostics 9 (2019) 3150.
[118] B. Li, X. Wang, L. Chen, Y. Zhou, W. Dang, J. Chang, C. Wu, Theranostics 8 (2018) 4086.
[119] Z. Wang, Y. Fu, Z. Kang, X. Liu, N. Chen, Q. Wang, Y. Tu, L. Wang, S. Song, D. Ling, H. Song, X. Kong, C. Fan, J. Am. Chem. Soc. 139 (2017) 15784–15791.
[120] Y. Li, K. Zhang, P. Liu, M. Chen, Y. Zhong, Q. Ye, M.Q. Wei, H. Zhao, Z. Tang, Adv. Mater. (2019) 1901570.
[121] X.-G. Wang, Z.-Y. Dong, H. Cheng, S.-S. Wan, W.-H. Chen, M.-Z. Zou, J.-W. Huo, H.-X. Deng, X.-Z. Zhang, Nanoscale 7 (2015) 16061–16070.
[122] J. Liu, T. Liu, P. Du, L. Zhang, J. Lei, Angew. Chem. 131 (2019) 7890–7894.
[123] X. Lian, Y. Huang, Y. Zhu, Y. Fang, R. Zhao, E. Joseph, J. Li, J.P. Pellois, H.C. Zhou, Angew. Chem. Int. Ed. 57 (2018) 5725–5730.